Manufacturing method and experimental validation for a zero-stiffness compliant mechanism as a flexible head support

May 23, 2020

Sander Kempen 4328124
Coaches: Giuseppe Radaelli &
Ali Amoozandeh Nobaveh
TU Delft

Content

Introduction

A novel concept for a zero torsional stiffness spatial compliant mechanism as a head support was developed by researchers at the TU delft. This design introduces a mechanism that reduces the torsional stiffness while retaining the bending stiffness of the mechanism. The proposed zero stiffness concept is based on prestressing two elastic beams. The two beams are shaped around the back of the head of the wearer, and becomes extremely compliant in torsion due to the prestress between the beams. This enables rotation of the head while still stabilising the head. The two beams of the design are I-shaped with a wall thickness of 1 mm, curved in one plane and were made from polycarbonate. The design parameters of the design were tuned using a Finite Element Analysis of the model to achieve a rotational moment as low as possible.

A large reduction in rotational stiffness of the mechanism was observed in experiments. However, polycarbonate is probably unsuited for the mechanism for the intended long term use. Instead high strength metal could be used. High strength metals are often used in planar compliant mechanisms due to their high yield strength and their creep resistance. However, manufacturing methods to produce spatially curved beams made of high strength metal and thus suitable for the mechanisms have not been found in literature. The focus of this research is to present a new method of manufacturing for the two beams of the mechanism which are made from high strength steel. The beams were partially redesigned to be better suited for the proposed manufacturing method where the original finite element analyses of the design was used.

The report consists of a paper and an appendix. The paper with the title "Manufacturing method and experimental validation for a zero-stiffness compliant mechanism as a flexible head support" presents a clear overview of the research. The appendix contains more detailed and extended information on some of the subjects in the paper.

Manufacturing method and experimental validation for a zero-stiffness compliant mechanism as a flexible head support

Sander Kempen

Faculty of Mechanical, Maritime and Materials Engineering

Department of Precision and Microsystems Engineering (PME)

Giuseppe Radaelli, Ali Amoozandeh Nobaveh and Just Herder

May 23, 2021

ABSTRACT

This paper presents a manufacturing method for a zero-stiffness compliant mechanism to be used as a flexible head support. The manufactured design consists of two curved, thin-walled U-beams made of high strength steel. The beams are prestressed in opposite directions to obtain zero torsional stiffness so that rotation of the head is allowed. The presented manufacturing method for the beams consists of three different steps; (1)Production of a straight U-beam using a saw mill, (2)Bending the U-beam with a bending tool based on press die forming, (3)Heat treatment to increase the strength of the profile.

C75 high strength steel is used for the production of the beams. The straight U-beams with a wall thickness of 0.4 mm were produced within an accuracy of 0.03 mm. The formed U-beams in step 2 approximately follow the desired curve with a maximum lateral error of 1mm which is deemed sufficient for this application. Finally, the beams were strengthened using a standard quenching and tempering heat treatment which increased the yield strength with a factor of 4 up to 1650 MPa. A prototype was made which consists of a 3D printed lower and upper base, as well as two prestressed curved U-beams produced with the presented manufacturing method. The performance of the compliant mechanism design with the produced beams is analysed in terms of the moment-angle curve. Prestressing reduced the maximum moment between -60 and 60 degrees with a factor of about 60 to 0.015 Nm.

Keywords: Compliant mechanism, zero stiffness, head support, manufacturing method, springback

1. INTRODUCTION

Patients with pareses such as Duchenne Muscular Dystrophy(DMD) gradually lose control and strength of their neck and shoulder muscles and at some point during the development of the disease become unable to stabilise and move their head [1]. This impedes their performance during daily activities as these almost always involve visual feedback. As a result, they need an assistive device that would stabilise their head as well as allow movements in order to improve functional performance. Current solutions are either bulky and restrain the head for all movements[2,3] or only allow rotation of the head[4,5].

To achieve stabilisation without constraining the natural movement of the head, a zero-stiffness three-dimensional compliant mechanism concept has been developed by researchers at the TU Delft which stabilises the head while still leaving rotation possible. The concept consists of two compliant beams curved around the back of the head. Zero stiffness in rotation is achieved by prestressing the two compliant beams in opposite directions. The beams are designed to be U-shaped with a wall thickness of 0.4 mm, curved in one plane and made of high strength steel. A special manufacturing method is required to produce the beams for the head support. Figure 1 shows the concept with the curved beams in unstressed state.

Compliant mechanisms are increasingly popular in multiple fields of application. Designers become more familiar with their potential benefits, most frequently mentioned of which are low friction, no wear, no need for lubrication, no backlash and easy assembly[7]. By far, most compliant mechanisms used today were conceived as a planar mechanism. However, increased attention and interest for three-dimensional compliant mechanisms is foreseen in the near future[8]. Due to the relatively new research field, limited literature is available for manufacturing methods of three-dimensional compliant mechanism made out of metal.

Additive manufacturing, especially powder bed fusion, is used for three-dimensional compliant mechanisms made out of metal[9, 10]. A minimum wall thickness of 0.75 mm is advised for flexures[11], since the removal of support material from thin-walled structures is problematic and the strength of the metal that can be achieved is not high enough for this application despite recent developments[12].

CNC milling can be used to produce curved U-beams from a metal sheet. A small end mill with a diameter of only 1.5 mm is required to manufacture the gap in the U-beam between the two flanges. A problem with this method is that these small end mills are very fragile and tend to break quickly, leading to defects in the material. On top of that, a lot of material is wasted due to the curve of the beam and the process is very time consuming.

Hydroforming, crash forming and draw forming can produce complex profile shapes by pushing a metal sheet in a three-dimensional mould. However, residual stresses cause various springback defects for these techniques such as: opening angle, wall warp, torsion, camber, and buckling torsion[13]. Also, thinning of the sheet material is an issue[14].

Current manufacturing techniques are not suitable to produce the required thin-walled curved beams made of high strength steel. The combination of thin-walled U-beams, curved in one plane and made from high strength metal makes it very challenging to produce. A manufacturing method is proposed to produce the beams designed for a compliant mechanism as a head support. The proposed method can also be used for other cross section shapes, dimensions and curvatures to

produce beams for other applications making this method interesting for other purposes in the field of three-dimensional compliant mechanisms.

   The goal of this paper is to present and analyse a manufacturing method for the curved steel beams of a zero-stiffness distributed compliant mechanism for a flexible head support. The U-shaped beams are curved in only one plane and are made from high strength C75 steel. The manufacturing method consists of the following three steps.
1. Production of a straight U-beam using a saw mill
2. Bending the U-beam with a bending tool based on press die forming
3. Heat treatment to increase the strength of the profile

   Each step is validated experimentally. Finally, the performance of the compliant mechanism design with the produced beams is analysed. The design consists of a lower and upper base connected by two beams. A detailed analysis for the lower and upper base is left out of the scope of this paper. The focus is placed upon presenting a manufacturing method for the curved, thin-walled U-beams made of high strength steel and an analysis of the performance of the beam in the design.
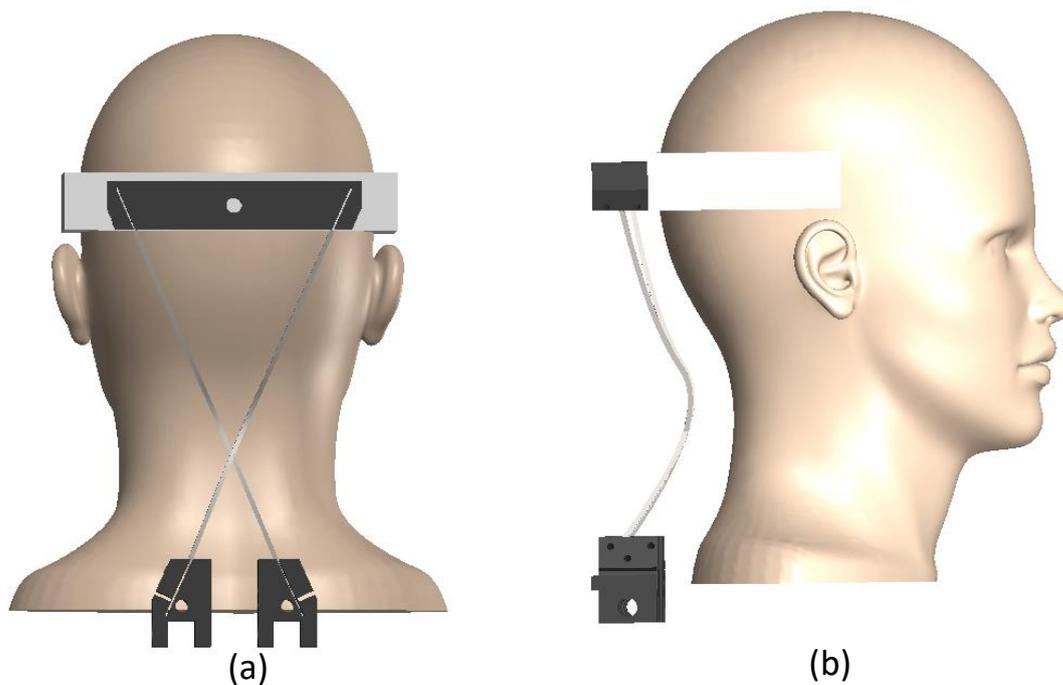
Figure 1. *Design of the zero-stiffness compliant mechanism as a head support in unstressed state with:(a) Back view and (b) Side view*

2. DESIGN

Patients with pareses such as DMD lose function in their neck and shoulder muscles and they require support and stabilisation of their head while rotation should still be possible. Researchers at the TU Delft have developed a novel concept of a zero-stiffness compliant mechanism as a head support for this problem.

Three design requirements of the head support are stated:
- The device volume should be contained at an offset of no more than 10 cm from the body contour and should not obstruct the field of vision.
- The device should allow the possibility of head movement in the direction of flexion-extension (for looking up and down, eating, drinking etc.) and head rotation along the vertical axis (looking left and right).
- The device should have a very low resistance in rotation between looking straight ahead and rotating the head 60 degrees along the vertical axis in both the left and right directions.

The working principle of the design is based on a zero-stiffness mechanism which is achieved by prestressing two elastic beams in opposite directions. Figure 2(a) shows the rear view of the undeformed beams connected under an angle α to the lower and upper body. Figure 2(b) shows the prestressed beams where prestress is achieved by swapping the position of the lower ends of the beams. By tuning both the dominant positive torsional stiffness of the beams and the negative stiffness of the beams created by the prestress, a bi-stable mechanism with a very low moment could be achieved. Beams with a relatively high bending stiffness and low torsional stiffness can yield this desired balance.
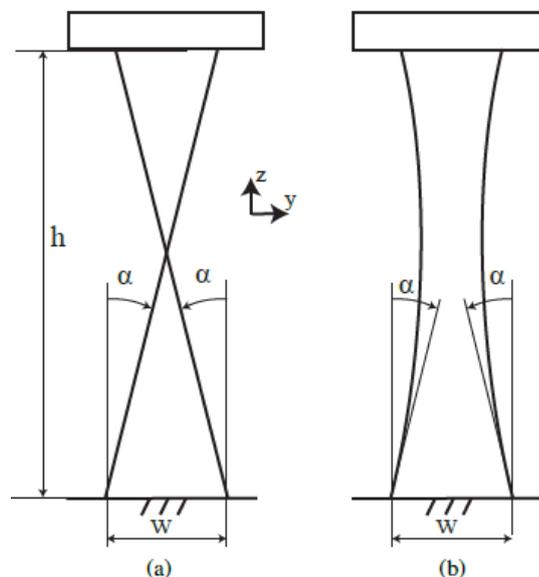
Figure 2. *(a) Rear view of the undeformed beams and connecting upper body. (b) Prestress is applied by swapping the clamped ends of the beams, while holding the orientation of the connecting body. and without twisting the beams.*

A U-shaped cross section was chosen for the beams, since this fulfils the required high bending stiffness and low torsional stiffness and also has the advantage for the manufacturing method over other cross sections which is discussed in Section 3. The beams are shaped around the head of the wearer so that it follows the body contour within the 10 cm offset of the body as stated previously in the requirements. Also, the curvature of the beams is designed for the mechanism such that the top body approximately follows the path of the head when rotating. The beams are curved in only one plane, as illustrated in Figure 3. High-strength steel is chosen as the material for the beams because of the high creep resistance, fatigue strength and elastic deformability of this material which is required due to the large deformation and constant prestressing of the beams.

Side view:

187,3mm

Front view:

Cross-section:

Ц
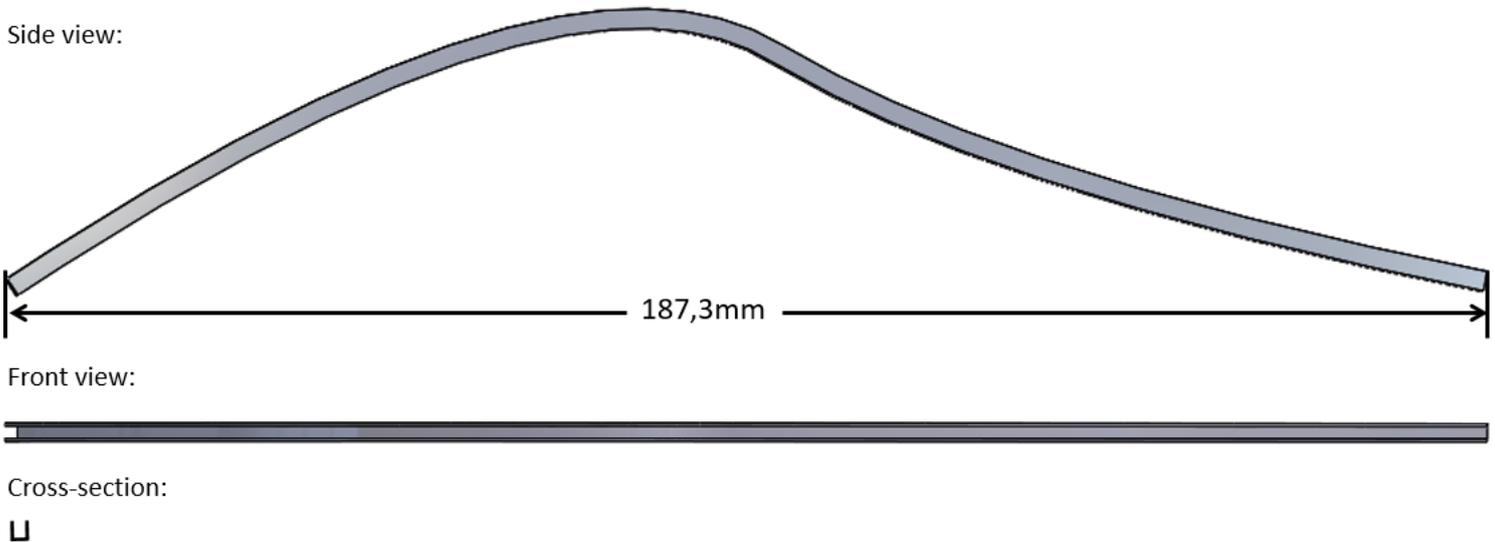
Figure 3. *Side view, front view and cross section of the curved U-beam on scale 1:1*

 A custom Finite Element Analysis(FEA) of the model is implemented in MATLAB to tune the design parameters such that the rotational moment is minimised. The model is a 3D co-rotational beam formulation based on the work of Battini [15]. The constitutive material law is linear, warping effects are not considered, and shear is not accounted for. First, the system is prestressed in the simulation by swapping the position and inclination of the two legs without applying any torsion on the beams. After the prestress step, a rotation of 60 degrees in the vertical direction is applied on the connecting upper body about a non-fixed axis. Then a rotation of -120 degrees is applied to obtain the moment characteristics from 60 to -60 degrees. The rotation is applied in 100 equal steps. It is assumed that no other external loads are acting on the system.

   The design parameters that can be tuned to achieve the desired balance are the following.
   - The dimensions of the U-cross section: H, B, t_f, t_w (Figure 4)
   - The inclination angle α (Figure 2)
   - The leg width w (Figure 2)

Figure 4 shows the material properties used in the analyses and the design parameters chosen which result in a minimised rotational moment. The tuned moment characteristic of the FEA simulation is shown in Figure 5 .

The resulted design parameters and material properties were used to perform a static structural stress analysis in Ansys to determine the maximum stress in the beam. The analysis showed a peak of 1450 MPa at the lower end of the beam. The following section presents a manufacturing method to produce the beams with the required dimensions of the U-section, curve of the beam and strength of the steel.

Design parameters

H=2.52 mm
B=2.4 mm
t_w=0.4 mm
t_f=0.4 mm

W=50 mm
α= 23,5°

Material properties

E = 210GPa
G = 81GPa
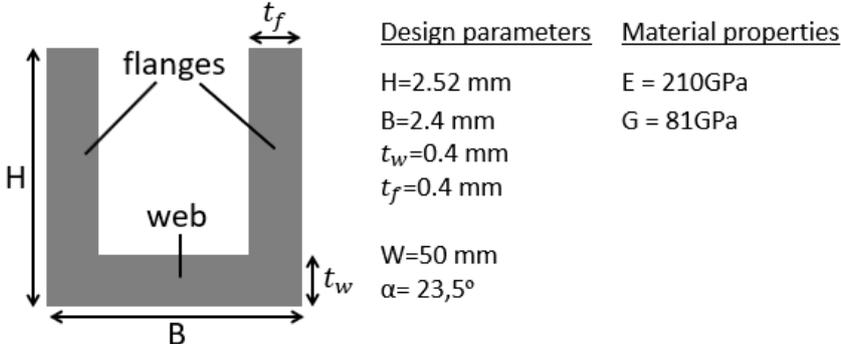
Figure 4: *Design parameters of the design includes the dimensions of the U-cross section, the inclination angle α and the leg width W. The material properties of steel used in the model are shown on the right.*
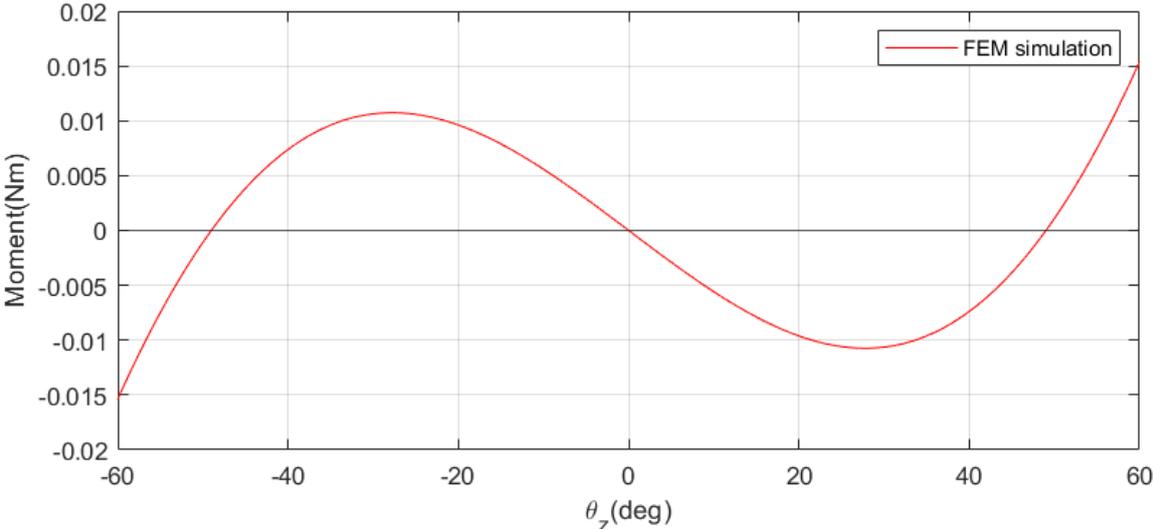
Figure 5. *The moment characteristic of the rotational movement of the mechanism which is a result of a Finite Element Analyses.*

3. METHOD

3.1 General manufacturing process

The proposed manufacturing method to produce thin-walled, curved U-beams out of steel consists of the following three steps.
1. Production of a straight U-beam using a saw milling machine
2. Bending the straight U-beam using a dedicated bending tool based on matched die forming
3. Strengthening the steel curved U-beam with heat treatment

Keeping the costs of the manufacturing method low to ensure the head support is affordable directly influenced the choices made in each step. High carbon C75 steel was chosen for the beams since it is accessible on the market, relatively cheap for a high strength steel and C75 can reach strengths of 1900 MPa after heat treatment.

3.2 Straight U-beam production

The first step of the production method is to produce a straight U-beam from a 3 mm C75 steel plate. A milling machine was used to produce the U shape. The steel plate was clamped to the bed of the milling machine with two clamping mechanisms, one on each side, as shown in Figure 7. First, the desired profile height of 2.52 mm is achieved by removing part A (Figure 6) over the full length of the steel plate with a plain milling cutter. Next, a slitting saw, a flat circular shaped tool with small teeth on the outer diameter, was used on the same milling machine to remove parts B, C and D of Figure 6. A slitting saw has several advantages over a normal end mill: the heat generation is lower which prevents thermal deflection of the material, there is much less chance of mill breakage and it is less time consuming. The slitting saw used had a thickness of 1.2 mm, a diameter of 75 mm and the rotational speed of the milling machine was set to 220 rpm. The parts B, C and D were removed in this order in 0.2mm deep increments over the full length of the plate. Finally, the beams were cut to a length slightly longer than required using a grinder, after which the excess was removed with a belt sander to obtain the correct length.
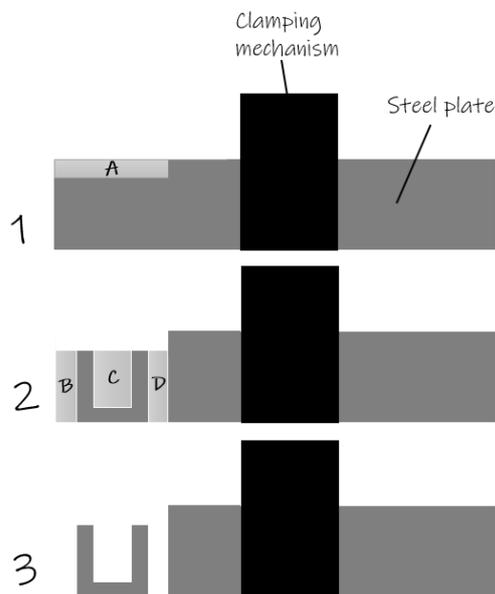
Figure 6. *Steps of the milling process where a U-beam is milled from a metal plate. First part A is removed with an end mill cutter, and then parts B, C and D are removed with a slitting saw.*

Figure 7. *The setup of the milling machine where the steel plate is clamped to the bed with 2 clamping mechanisms.*

3.3 Bending U-beam

3.3.1 Bending method

The second step of the manufacturing method is to bend the U-beam to the required curvature. Matched die forming is a technique in which sheet material is placed between two matched dies which are pressed together with a large force to form the sheet (Figure 8). This principle is used to form the straight U-beam to the desired curvature.

After unloading the matched dies, the formed metal tends to partially return to the original shape due to elastic recovery of the material. This phenomenon is referred to as the springback. One way to compensate for the springback is by overbending the material. Two methods are commonly used to determine a suitable die shape which compensates for springback: the trial-and-error method and the Finite Element Method(FEM) based on an iterative procedure[15]. The trial-and error method is a very time-consuming process and the entire method has to be repeated if a different curvature is required in future. The FE methods based on an iterative procedure requires relatively long execution times. Also, another downside to using FE methods is that it does not give insights in the springback behaviour of a U-section. Instead, a new analytical method is proposed in Section 3.3.2 to determine a die shape which compensates for springback.

A relatively small force is required to form U-beams due to the small dimensions of the cross section. For this reason a simple bending tool could be designed and produced to form the U-beam with the computed matched dies. This bending tool is described in Section 3.3.3.
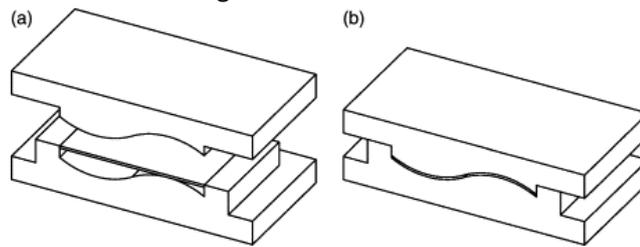
Figure 8. *Illustration of matched die forming for a sheet in unloaded position(a) and in Loaded position(b).*

3.3.2 Die design method

A new analytical method is introduced to compute the die shape which compensates for springback. The method determines the radius of curvature which compensates for springback at a large number of nodes on the curve path of the beam and uses these radii to determine the curvature of the die. The method consists of three steps.

1. The curve path of the beam is discretized and the radius of curvature R_O is calculated for every node
2. Using the radius of curvature found in step 1, the new radius of curvature which compensates for springback R_S is calculated for every node
3. The curve of the die can be calculated with radius R_S which compensates for the springback found in step 2 at every node

(1) *Radius of curvature at node*

The radius of curvature R_O at node $P(i)$ can be determined by calculating the radius of the circle that goes through $P(i)$ and the two neighbouring nodes $P(i-1)$ and $P(i+1)$. If the number of nodes is large enough, it can be assumed that the radius R_O of the circle that coincides with nodes $P(i-1)$, $P(i)$ and $P(i+1)$ can be considered as the radius of curvature of the middle node $P(i)$,

see Figure 9. The radius of curvature of the circle can be calculated using the inverse of the Menger curvature[16].

$$R_o = \frac{a \cdot b \cdot c}{4 \cdot A} \tag{1}$$

Where the side lengths a, b and c can be calculated using the cartesian distance formula as follows.

$$a = \sqrt{(x_i - x_{i-1})^2 + (y_i - y_{i-1})^2} \tag{2a}$$
$$b = \sqrt{(x_{i+1} - x_i)^2 + (y_{i+1} - y_i)^2} \tag{2b}$$
$$c = \sqrt{(x_{i-1} - x_{i+1})^2 + (y_{i-1} - y_{i+1})^2} \tag{2c}$$

The area A of the triangle with the sides a, b and c can be calculated using Heron's formula,

$$A = \sqrt{s(s-a)(s-b)(s-c)} \tag{3}$$

where s is the semi-perimeter of the triangle, that is:

$$s = \frac{a+b+c}{2} \tag{4}$$
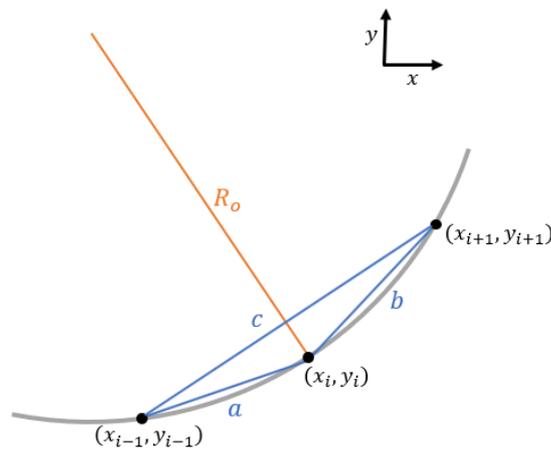
Figure 9. *Schematic of a circle with radius of curvature R_O that goes through nodes $P(i-1)$, $P(i)$ and $P(i+1)$.*

(2) Springback at a node

The radius of curvature that compensates for springback at each node is determined by predicting the springback of a U-section under bending. The springback values have been determined with the assumptions of yielding according to von Mises criteria and is based on the work of Saleh et al.(2018).

Figure 10 shows the relation between the applied bending moments on the U-section and the change in curvature. At point A the material yields and at the maximum bending moment the material undergoes plastic deformation. At point B, when the applied moment is released, elastic springback occurs from point B to point C. The change in curvature after bending due to elastic springback is given by the following equation

$$\frac{1}{R_f} - \frac{1}{R_0} = \frac{M_{max}}{\partial M_e / \partial(1/R)} \tag{5}$$

Where R_0 is the bending radius, R_f is the final radius after springback occurs, M_{max} the applied moment and M_e the moment in the elastic range.
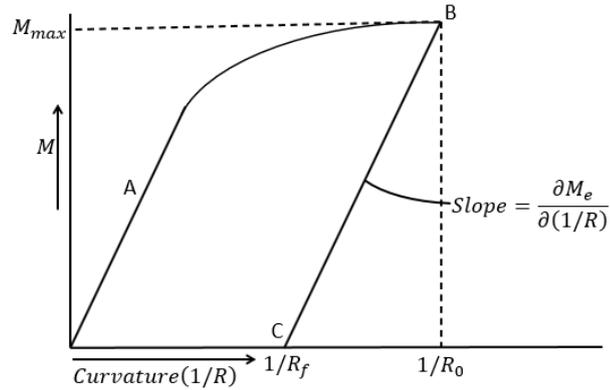
Figure 10. *Relation between applied bending moment and curvature.*

Figure 11 illustrates the U-section of the beam with the z-axis positioned at the neutral axis of the U-section where the bending strain is zero. The bending strain in the x-direction, ε_x, increases linearly with the distance along the y-axis from the neutral axis and can be written as follows.

$$\varepsilon_x = \frac{y}{R_o} \tag{6}$$

The approximate bending stress in the elastic region following von Mises criteria can be written as

$$\sigma_{x,e} = \frac{E}{(1-v^2)} \varepsilon_x \tag{7}$$

and the bending stress in the plastic region following von Mises criteria can be written as

$$\sigma_{p,e} = \frac{K}{\left(\frac{3}{4}\right)^{\frac{1+n}{2}}} \varepsilon_x{}^n, \tag{8}$$

where K is the strength coefficient and n is the strain hardening exponent.
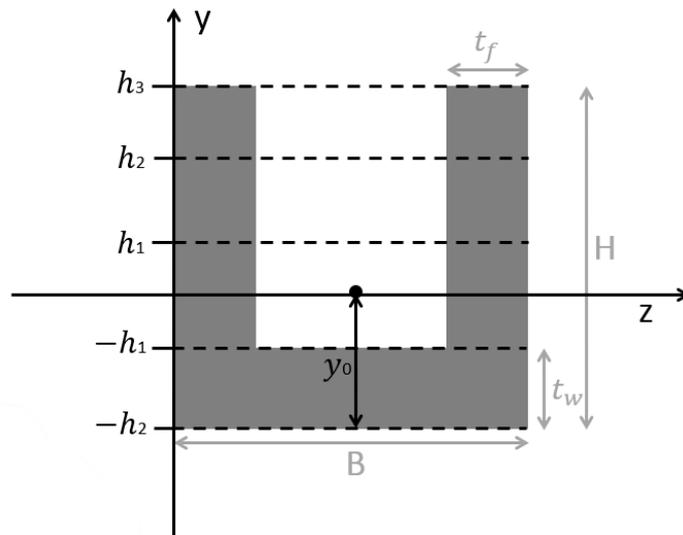
Figure 11. *U-section of the beam where the z-axis is positioned at the neutral axis.*

The springback behaviour of the U-section depends on the position of the yield point (h^*), which is the distance from the neutral axis up to the layer at which the yielding occurs. The position of the yield point h^* can be written as follows.

$$h^* = R_0 \left(\frac{K}{E}\right)^{\frac{1}{1-n}} \left(\frac{1-v^2}{\sqrt{1+v^2}-v}\right)$$

(9)

The applied bending moment M_{max} is analysed for three cases in which the position of the yield point h^* differs along the height of the beam. Case (1), where the yield point h^* is in the upper part of the flange of the U-section between h_2 and h_3. Case (2), where the yield point h^* is in the web of the U-section between h_1 and h_2. And Case (3), where the yield point h^* is between the neutral axis and the web of the U-section which is between the neutral axis and h_1.

The heights h_1, h_2 and h_3 (Figure 11) can be expressed in terms of the centroid distance y_o, which is the distance from the neutral axis to the bottom of the U-section.

$$h_1 = y_o - t_w$$ (10a)
$$h_2 = y_o$$ (10b)
$$h_3 = H - y_o$$ (10c)

The centroid distance y_o can be expressed using the dimensions of the U-section

$$y_o = \frac{1}{A}\left(\frac{(B-2\cdot t_f)\cdot t_w^2}{2} + t_f \cdot H^2\right),$$

(11)

where the area A of the U-section is given in the following equation.

$$A = 2 \cdot H \cdot t_f + (B - 2\cdot t_f) \cdot t_w$$

(12)

The bending moment can be written for the previously mentioned three cases:
Case (1), where the yield point h^* is in the upper part of the flange of the U-section between h_2 and h_3.

$$M_{max} = 2\left(\int_0^{h1} \sigma_{x,e} \cdot 2 \cdot t_f \cdot y \cdot dy\right) + \int_{h1}^{h2} \sigma_{x,e}\left(2 \cdot t_f \cdot y + B \cdot y\right)dy$$

(13)

$$+ \left(\int_{h2}^{h*} \sigma_{x,e} \cdot 2 \cdot t_f \cdot y \cdot dy\right) + \left(\int_{h*}^{h3} \sigma_{p,e} \cdot 2 \cdot t_f \cdot y \cdot dy\right)$$

Case (2), where the yield point h^* is in the web of the U-section between h_1 and h_2.

$$M_{max} = 2\left(\int_0^{h1} \sigma_{x,e} \cdot 2 \cdot t_f \cdot y \cdot dy\right) + \int_{h1}^{h*} \sigma_{x,e}\left(2 \cdot t_f \cdot y + B \cdot y\right)dy$$

(14)

$$+ \int_{h*}^{h2} \sigma_{p,e}\left(2 \cdot t_f \cdot y + B \cdot y\right)dy + \left(\int_{h2}^{h3} \sigma_{p,e} \cdot 2 \cdot t_f \cdot y \cdot dy\right)$$

Case (3), where the yield point h^* is between the neutral axis and the web of the U-section which is below h_1.

$$M_{max} = 2\left(\int_0^{h*} \sigma_{x,e} \cdot 2 \cdot t_f \cdot y \cdot dy + \int_{h*}^{h1} \sigma_{p,e} \cdot 2 \cdot t_f \cdot y \cdot dy\right)$$

(15)

$$+ \int_{h1}^{h2} \sigma_{p,e}\left(2 \cdot t_f \cdot y + B \cdot y\right)dy + \left(\int_{h2}^{h3} \sigma_{p,e} \cdot 2 \cdot t_f \cdot y \cdot dy\right)$$

The moment M_e in the elastic range of the springback equation (5) can simply be written as the bending equation

$$M_e = \frac{\sigma_{x,e} \cdot I_z}{y},$$

(16)

where I_z is the moment of inertia about the neutral z-axis of the U-section.

$$I_z = \frac{2 \cdot t_f \cdot H^3 + (B - 2 \cdot t_f) \cdot t_w{}^3}{3} - A \cdot y_o$$

(17)

Finally, equation (16) and the equations (14, 15 and 16) for the three cases dependent on the height of the yield point h^* (10a, 10b or 10c) can be substituted into equation (5). The radius of curvature R_O which is the radius that compensates for springback, can be calculated by solving equation (5) for the desired final radius of curvature R_f determined in step 1 of the die design method.

(3) Curve of the die shape

The shape of the die can be determined by continuously predicting the next node $P(i + 1)$ using the two previous nodes $P(i - 1)$ and $P(i)$, the length of the sides a and b determined in step 1, and the radius of curvature R_S at $P(i)$ calculated in step 2. The same assumption is made as in step 1, that for a large number of nodes, the circle with radius R_S that goes through nodes $P(i - 1)$ and $P(i)$, also goes through node $P(i + 1)$.

Figure 12 illustrates a schematic overview of the situation described where angles α_1 and α_2 can be determined using an isosceles triangle with equal sides of length R_S and side a to calculate α_1, and side b for α_2 .

$$\alpha_1 = \cos^{-1}\left(\frac{\frac{a}{2}}{R_S}\right)$$

(18)

$$\alpha_2 = \cos^{-1}\left(\frac{\frac{b}{2}}{R_S}\right)$$

(19)

The angles β_1 and β_2 shown in Figure 10 can be determined using the following geometric equations.

$$\beta_1 = \tan^{-1}\left(\frac{y_i - y_{i-1}}{x_i - x_{i-1}}\right)$$

(20)

$$\beta_2 = \pi - \alpha_1 - \alpha_2$$

(21)

The angle γ is the summation of β_1 and β_2.

$$\gamma = \beta_1 + \beta_2$$

(22)

Finally, the predicted x and y coordinates of node $P(i + 1)$ can be expressed using the coordinates of $P(i)$, distance b and angle γ

$$x_{i+1} = x_i + b \cdot \cos(\gamma)$$

(23)

$$y_{i+1} = y_i + b \cdot \sin(\gamma)$$

(24)
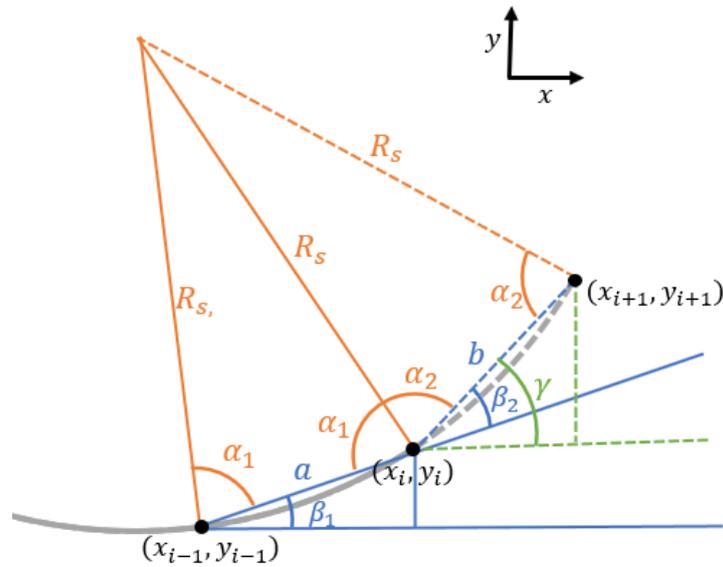
Figure 12. *Schematic of the radius R_s of the circle that goes through nodes $P(i-1), P(i)$ and $P(i+1)$.*

The described method is implemented in MATLAB to determine the shape of the die. It is assumed that the material has not been strain hardened, so that the strength coefficient equals the yield strength of 410 MPa. The strain hardening exponent has been estimated from similar materials to be 0.2. The other material properties and dimensions of the U-section used can be found in Figure 3.

Figure 13 shows the curve of the beam in blue and the curve of the die shape resulting from the implemented method in red.
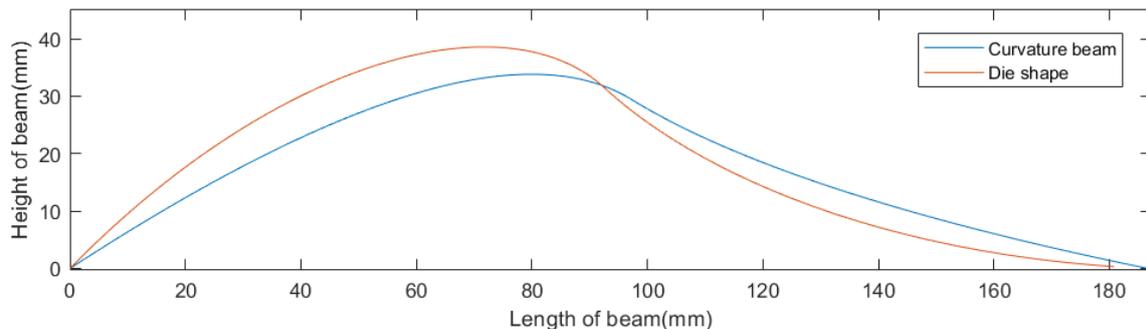
Figure 13. *The calculated die shape using the 3 step method implemented in MATLAB.*

3.3.3 Bending tool

A bending tool was developed to perform the matched die forming. Figure 14 shows the design of the bending tool. The 2.5 mm thick matched dies (A) are placed on two lower bases (B) made of PMMA. A 2 mm thick PMMA die holder (C) is mounted on both of the bases to prevent the die from moving in the horizontal direction. A PMMA plate (D) is placed on top of the dies and clamped with bolts to the base. This prevents the die from moving in the vertical direction and also works as a guidance for the U-beam when bending. Below both bases, two linear block bearings (E) which slide over two guide rails are mounted, such that only linear motion in the desired direction is possible when pressed together.

The dies were made of PLA using an Ultimaker 2.0 and the PMMA parts were laser cut. The straight steel U-beam can be placed on the top of the die because the open side of the U-beam fits perfectly thanks to the cutouts at the top and bottom of the die for the flanges. Both of the bases were pressed together tightly with a clamp to bend the U-beam, as shown in Figure 15.
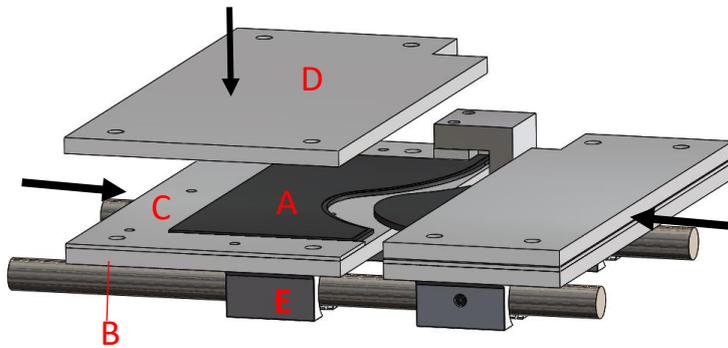
Figure 14. *Design of the bending tool. The two matched dies are shown in black.*

Figure 15. *The setup of the bending tool where a glue clamp is used to press both parts together.*

3.4 Heat treatment of curved U-beam

At this point, the beams are still in a relatively soft state since this is required for milling and bending the U-beam. However, the steel has the potential for a much greater strength. As discussed in the design, a high-strength steel is required. For this reason, it was chosen to strengthen the beams by performing a standard quenching and tempering heat treatment. The beams were hardened by austenitizing at 840 °C for about 2 minutes before being quenched in oil. The beams are very brittle after quenching and therefore tempering is required to increase the ductility. This improvement in ductility is however coupled with a decrease in yield strength. The effect of the tempering time mainly depends on the wall thickness of the material. An increase in tempering time results to an increase of ductility and a lower yield strength. So a compromise between ductility and yield strength has to be found. Therefore, multiple specimens with different tempering times were analysed which is discussed in Section 4.3. The beams were tempered at 480 °C which is a frequently used tempering temperature for C75 steel[18].

3.5 Experimental validation of the prototype

Figure 16(a) shows the assembled mechanism with two U-beams (A), connecting the upper body (B) and two lower clamps (C). The beams are produced using the manufacturing method explained previously. The connecting upper body and the two lower clamps are produced by 3D printing on an Ultimaker 2.0. The U-beams were form-fitted under an angle of 23.5° at the upper body and lower clamps, and clamped using two bolts. The lower clamps are 50 mm apart.

The assembled mechanism is analysed by measuring the moment and forces acting upon it during movement or rotation of the mechanism. The experimental setup is depicted in Figure 16(c). It consists of the head support with a 6 degrees of freedom (DOF) load cell (ATI mini40) (D) on the top of the connecting body to measure the forces and moments required to deflect the head support in a

certain position. A webcam (E) is used to track the position of the connecting upper body in the x-y plane and rotation around the z-axis. The mechanism is actuated slowly by hand using a handle (F) attached to the 6 DOF sensor.

The synchronisation in time of the force measurements and the position measurement is handled in LabVIEW and the Vision module. LabVIEW is set up to take a photo of the setup every 400 ms whereas the forces are measured every 50 ms. Since there are several force measurements for each photo, these are averaged at each position. Post processing is done in MATLAB using the Image processing toolbox; this resolves the orientation and position of the connecting upper body. Figure 16(b) shows a picture of the webcam with the orientation of the coordinate system used. The x-axis of the coordinate system is aligned with the profile attached to the base (G). The moment around the z-axis was measured when rotating from about -60 to 60 degrees in unstressed and prestressed state. The mechanism is left as free as possible in the other directions. The mechanism is actuated slowly by hand using the handle(F) in both experiments.

(a)

(b)

(c)
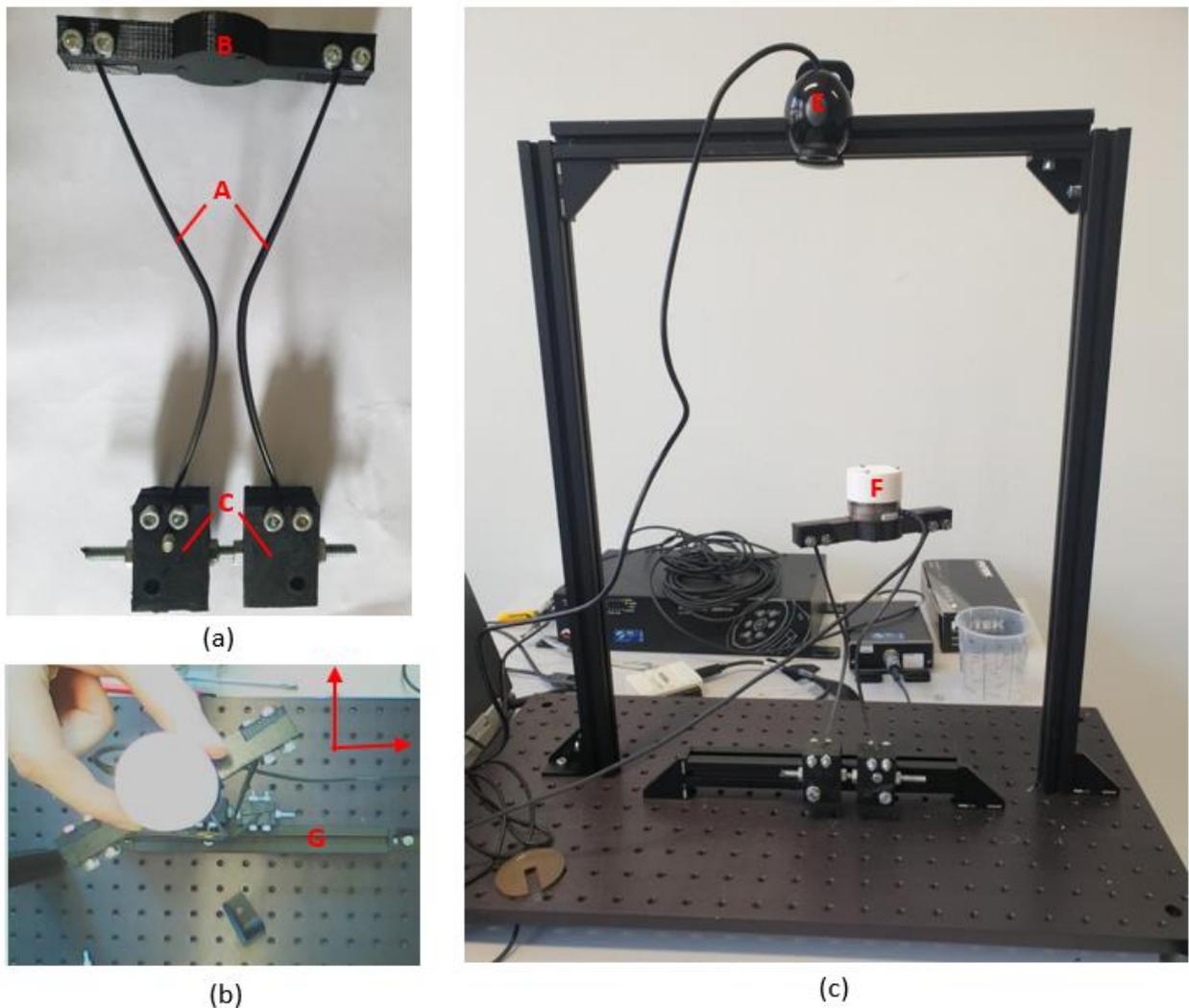
Figure 16. (a) *Experimental setup of the mechanism where a camera is used to determine the angle of the connecting top body and a 6 DOF sensor is used to measure the applied moment when rotating the mechanism by hand. (b) The assembled mechanism. (c) A picture made by the webcam during an experiment.*

4. RESULTS AND DISCUSSION

4.1 Production of a straight U-beam

Ten beams have been inspected visually and the dimensions of the beams have been measured. The horizontal surfaces of the U-beams have a good surface quality, while the vertical surfaces of the flanges are full of small scratches. The difference in surface quality is caused by the orientation of the saw mill. No significant effects of thermal deviation in the beam have been noticed.

Table 1 shows the required dimensions and the produced dimensions of the U-beam with their standard deviations. It can clearly be seen that a higher precision and accuracy was achieved for the horizontal dimensions B and t_f than for the vertical dimensions H and t_w. The likely reason for this difference is that the steel plate used was slightly hollow. The plate was clamped at both ends to the bed which mainly solved this problem. However, it is still likely that the plate was not perfectly straight. This resulted in a lower precision and accuracy over the length of the beam.

	Design(mm)	Produced(mm)
H	2,52	2,55±0,4
t_w	0,40	0,42±0,3
B	2,40	2,40±0,2
t_f	0,40	0,41±0,2

Table 1. *The U-section dimensions of the design and the produced dimensions with the standard deviation.*

4.2 Bending U-beam

Figure 17 shows the result of a beam which has been bent with the bending tool discussed in Section 3.3. It can be seen that the curvature of the U-beam almost perfectly follows the desired curvature which is shown with a black mold at an offset of 5 mm. Three beams have been analysed in detail. A picture of the curved beams was taken and analysed in MATLAB using the Image processing toolbox and the curvature of the beam could be reproduced by saving roughly 30 mouse click coordinates(x, y).

Figure 18(a) shows the mean curve of three beams with the standard deviation and the required curvature of the design. The figure shows that all the beams approximately follow the desired curvature of the design, but there are small deviations. Figure 18(b) shows the lateral bending error of the beam. The lateral bending error is defined as the deviation compared to the required curve of the beam in the lateral y-direction where both ends of the beams are positioned on the same line for both the measurements and the model. Figure 18(c) shows the comparison between the curvature of the design model and the average curvature of the produced beams along the length of the beam.

The curve of the beam has two main noticeable distortions: at the left end of the beam and at the transition from a positive to a negative curvature at the length of about 100mm. The distortion at the left side is possibly caused by the way the beam was cut to length. The U-beam was pushed against a belt sander to reduce the length of the beam until the required 200mm length was reached. The belt sander exerts a high positive force on the end of the beam which could have caused the

deflection. A detailed analysis of the distortion at the transition from a positive to a negative curvature has been left out of scope for this research.

Figure 17. *Result of a U-beam which is formed with the bending tool. The black mold shows the desired curvature at an offset of 5mm.*
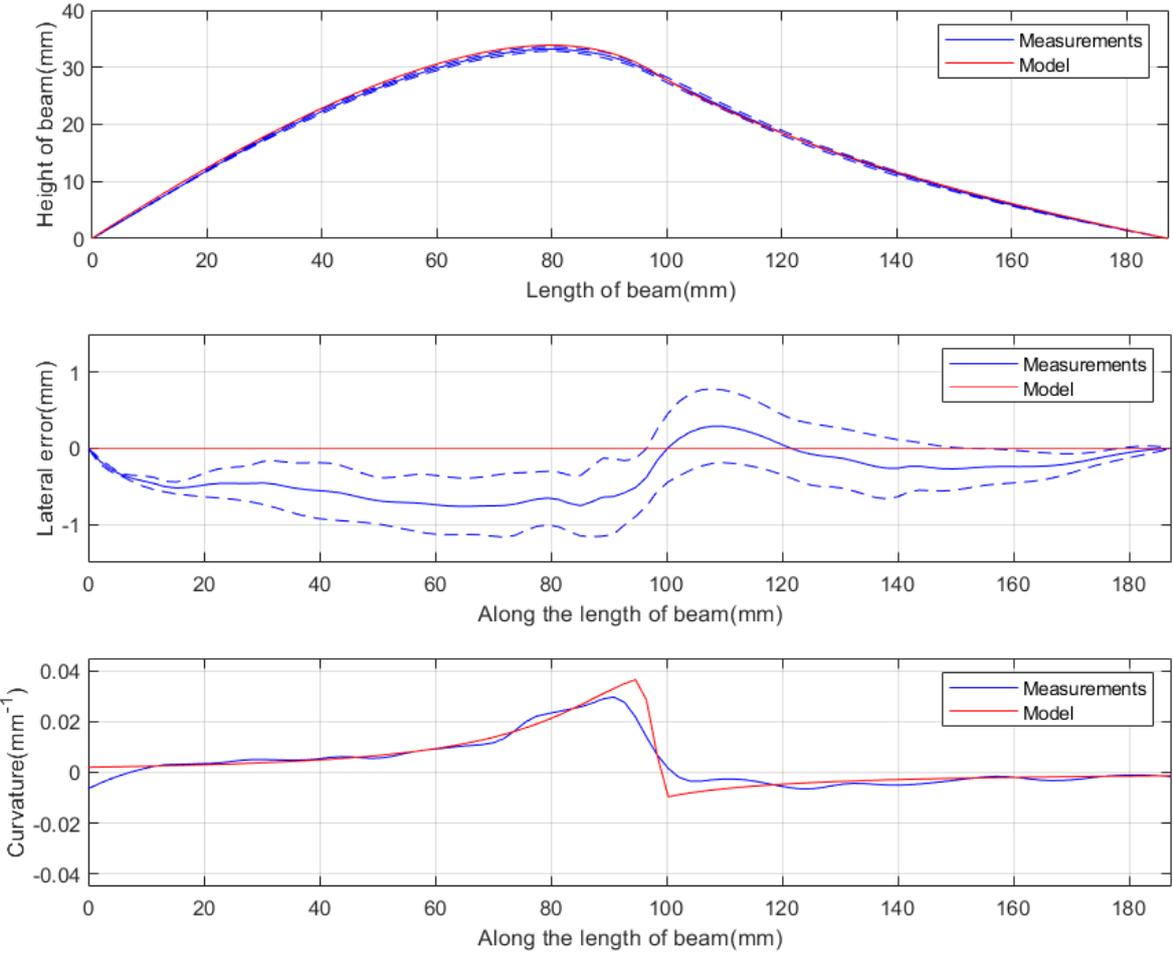
Figure 18. *(a) Average curve of three beams with the standard deviation and the desired curvature. (b)Average lateral bending error of the three beams. (c) Comparison between the curvature of the produced beams and the model.*

4.3 Heat treatment of curved U-beam

   The tempering time after quenching can be varied in order to result in different material properties. Six specimens have been analysed: in untreated state, quenched state and with four different tempering times after quenching. A three-point bending test was performed to analyse the load-displacement behaviour of the material. The U-beam was placed at the two supports with the flanges pointing downwards and the web at the top. The distance between the two support spans was 33 mm.

   Figure 19 shows the result of the bending test for the six specimens. An approximation for the yield strength is made for every specimen when the load per step has decreased by 5% with respect to the average load step, this indicates that yielding occurs in the top of the flanges. After quenching without tempering, the carbon steel is very brittle and breaks before yielding at about 1050 MPa. This indicates that tempering is required to increase the ductility which goes with a decrease in yield strength. After 30 seconds of tempering, the specimen breaks directly after yielding and has the highest yield strength of approximately 1800 MPa. However, the specimen is still very brittle and breaks just above the yield point. The material is unreliable, small microcracks in the material can quickly lead to failure below the yield strength. A tempering time of 90 seconds results in a small decrease in yield strength of about 150 MPa when compared to a tempering time of 30 seconds. However, the ductility and therefore the reliability of the material has increased massively. For this reason, a tempering time of 90 seconds was chosen for the prototype discussed in Section 4.4. Tempering times of 150 and 900 seconds show a further decrease in yield strength and an increase in ductility.

   The slope of the load-displacement curve in the elastic range, which is determined by the Young's modulus of the material is expected to be the same for every specimen. However, the slope of the lines change slightly for every specimen which is probably due to the small manufacturing errors of the U-beam discussed in Section 4.2.

   One of the two flanges on the U-beam breaks first, which results in the first decrease of the load. The remaining broken cross section can be considered as an L shape and can still absorb energy until the tensile strength is reached and the second flange breaks. This is the reason for the increase of the load after the first break which can clearly be seen for the tempering times of 30 and 90 seconds (blue and orange in Figure 19).
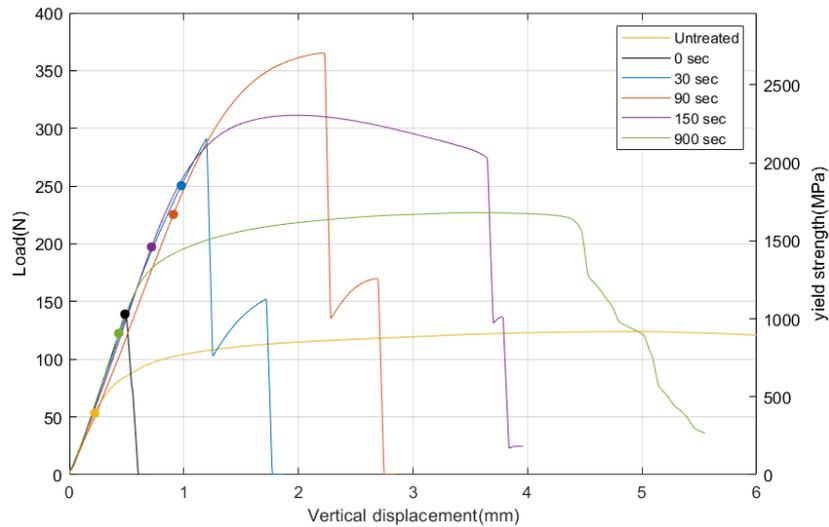
Figure 19. *Load-displacement curve of a three-point bending test for 5 quenched steel U-beams with variating tempering times and an untreated steel U-beam.*

The effect of the heat treatment on the curve has been analysed for three different beams. The curve for each beam is measured first in untreated state, then after quenching, and a third time after tempering the quenched beam for 90 seconds. The same method described in Section 4.2 is used by analysing a picture of the beam using the MATLAB image processing toolbox.

Figure 20(a) shows the mean of the curve of three beams in untreated state, after quenching and after tempering the quenched beam. It can be seen that the beams approximately follow the required curve of the beam for every state. No large deviations or warping effects were found on the curve or cross-section of the beam. Small deflections were noted in the lateral direction and are expressed in terms of the lateral bending error shown in Figures 20(b)-20(d) for each beam after every state. The computed curvature of the beam along its length resulted in a lot of noise and could not be used to analyse the deviation of the curve after quenching and tempering. This is probably a result of the inaccuracy of the mouse click coordinates. For this reason only the lateral bending error is used.

After quenching, the curve of the beams tends to deflect slightly in either direction. The direction and magnitude of the deflection differs per beam seemingly randomly. After tempering, the beams tend to partially spring back to the untreated state. This effect can be seen for all three of the beams.

The small deflections after quenching are most likely caused by the residual stresses in the material which is a common side effect of quenching steel[19]. Tempering slowly relieves the residual stresses in the material, so the longer the tempering time, the fewer residual stresses in the material. A tempering time of 90 seconds is relatively short which is probably the reason why the beam only partially returns to the original untreated shape.
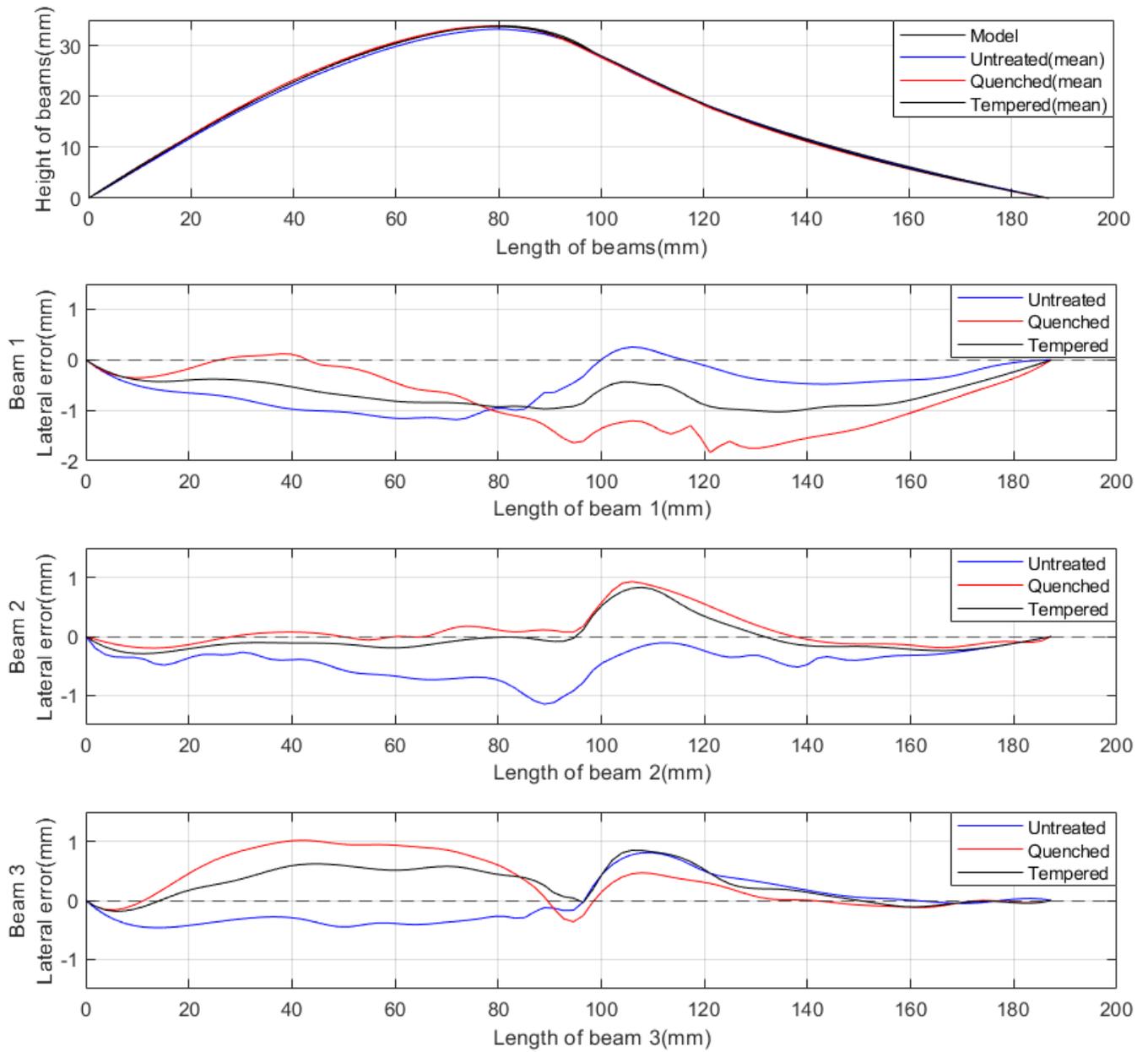
Figure 20. *(a) The average curve of the three beams in untreated state, after quenching and after tempering of the quenched beam. (b-d) Lateral bending error of beam 1-3 for the three different states.*

4.4 Experimental validation design

Figure 21 shows the result of the first experiment as explained in Section 3.5. A rotation was applied to the mechanism from -60 to 60 degrees in the prestressed state and a moment is applied from 0 to 60 degrees in the unstressed state. A curve is fitted through the raw data using the LOESS method. As predicted, prestressing the mechanism significantly lowers the rotational stiffness of the mechanism. The rotational stiffness is reduced by a factor of about 60. Moderate hysteresis was observed in both measurements, however an overall moment-angle-curve could still be obtained from the hysteresis loops with confidence.
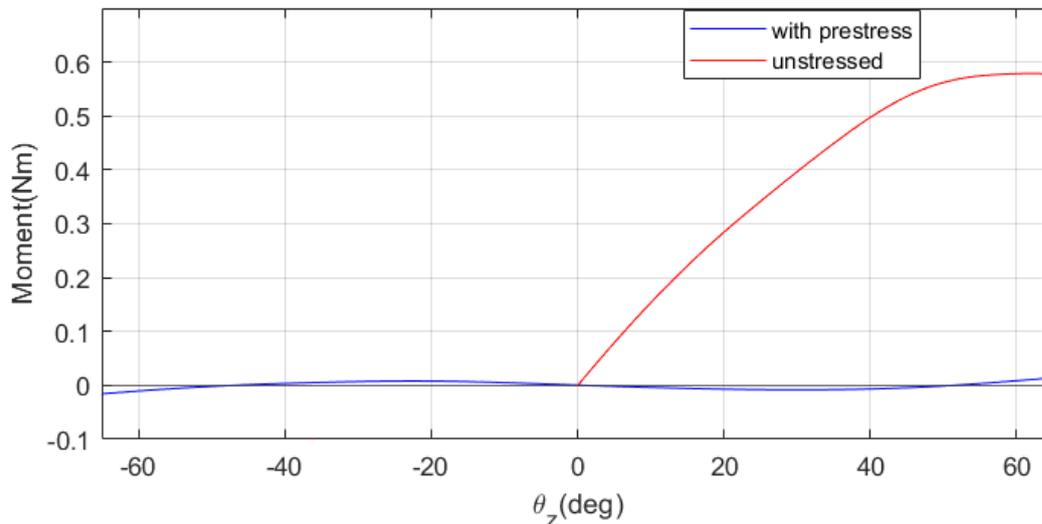
Figure 21. *The moment-angle curve of the unstressed and prestressed state of the compliant mechanism.*

Figure 22 shows a zoomed graph of the experiment in prestressed state including the hysteresis loop. Also, the simulated moment-angle curve of the FEA Model discussed in Section 2 is shown. It can be seen that both the experiment and the model had the same behavioural characteristics. However, the moment-angle curve of the experiment is stretched more widely which is in favour of the moment reduction between the -60 and 60 degrees. The figure shows that the assembled mechanism does not
exceed moments of 0.01 Nm in the range of -60 to 60 degrees, while the model has a maximum moment of 0.015 Nm at -60 to 60 degrees.

The hysteresis that was observed is moderate and this can be attributed to several factors. First, the clamping could be improved to reduce dissipation. The measurement errors and residual stresses in the material could have influenced the hysteresis loops seen in the results.

The hysteresis loop indicates that the system generates energy between -30 and 30 degrees, and dissipates energy above 30/-30 degrees. It is unlikely that energy is generated in the system.

The differences between the simulations and the experiment are likely caused by hardware, measurement and actuation error. Due to the manual actuation, the exact motion profile used in the simulation could not be replicated perfectly in the experiment. However, it is still the preferred accessible method to minimise any unwanted reaction forces during rotation.
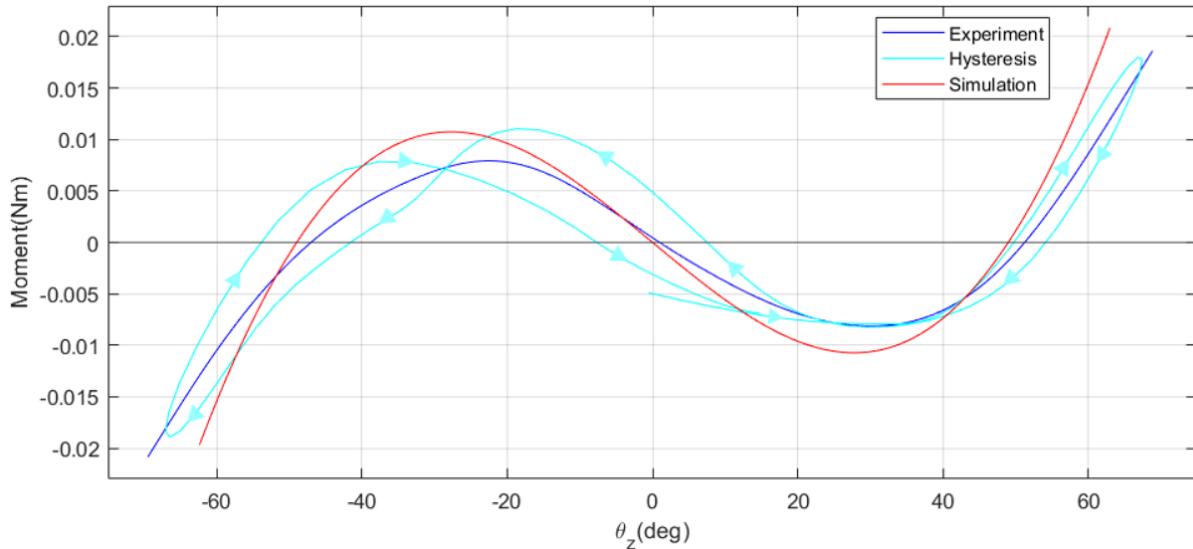
Figure 22. *The moment-angle curve of the experiment including the hysteresis. Also, the predicted curve of the simulation is shown.*

A reduction in performance was observed after the assembled prototype was in prestressed state for a couple of days. The observed bi-stability in the experiment disappeared and the maximum moment between -60 and 60 degrees increased by a factor of about 3. This is likely to be a result of creep in the material. An elaborate analysis of the effect of creep on the mechanism was left out of the scope of this research. However, creep and other forms of energy dissipation must be taken into account under the intended long term use conditions. The effect of creep can be reduced by increasing the yield strength of the material or by reducing the peak stresses in the prestressed beams.

Furthermore, an extensive study of the fatigue life was not performed. However, this should be taken into account for the intended long term use conditions.

5. CONCLUSION

This paper presents a manufacturing method for curved, thin-walled U-beams made out of high strength steel used in a zero-stiffness compliant mechanism as a flexible head support. The method consists of three steps: (1) Production of a straight U-beam using a saw mill, (2) Bending the U-beam with a bending tool based on press die forming, and (3) Heat treatment to increase the strength of the profile. The following conclusions were made:

- Thin-walled straight U-beams were produced using a saw mill within an accuracy of 0.03 mm
- U-beams were successfully bent using a dedicated bending tool based on matched die forming. A new die design method which compensates for springback was introduced.
- The curved beams were strengthened using a standard quenching and tempering heat treatment which increased the yield strength with a factor of about 4 up to 1650 MPa. No large deformations were observed after the heat treatment.

- Prestressing the mechanism lowers the rotational stiffness by a factor of about 60 which is also predicted using an FEA simulation. The fabricated mechanism has the same moment characteristics as the simulation.
- A reduction in performance was observed after the mechanism was in prestressed state for several days. This is most likely caused by creep at the lower and upper ends of the beam.

6. REFERENCES

[1] E. M. Yiu and A. J. Kornberg, "Duchenne muscular dystrophy", Journal of Paediatrics and Child Health, vol. 51, no. 8, pp. 759–764,Aug. 2015.

[2] "Papillon j Focal Meditech." [Online]. Available:http://www.focalmeditech.nl/nl/content/papillon

[3] "The Savant Headrest." [Online]. Available: http://www.symmetricdesigns.com/the-savant-headrest.html

[4] "Headpod j Patented system of Dynamic Head Support for people with loss of head control." [Online]. Available: http://www.headpod.com/

[5] "Axion Rotating Headrest Interface." [Online]. Available:http://www.symmetric-designs.com/axion-rotating-headrestinterface.html#axionhome

[7] L. L. Howell, "Compliant Mechanisms". New York, US: John Wiley and Sons Inc., 2001.

[8] G. Radealli, J.L. Herder, "Gravity balanced compliant shell mechanism, Int. J. Solids Struct. 118-119, 78-88. 2017.

[9] Merriam, E.G., J. E. Jones , S. P. Magleby , and L. L. Howell, "Monolithic 2 DOF fully compliant space pointing mechanism". Dept. of Mechanical Engineering, Brigham Young University. 2013.

[10] Ezekiel, E. G., Jones, E., and L. L. Howell. "Design of 3D-Printed Titanium Compliant Mechanisms"

[11] Merriam, E. G., Jones, J. E., and Howell, L. L., "Design of 3D-Printed Titanium Compliant Mechanisms". In Proceedings of the 42nd Aerospace Mechanisms Symposium. 2014.

[12] Kiener, L., Saudan,H., Perruchoud,G., Kruis,J., "Compliant Mechanisms Re-Design based on Additive Manufacturing and Topology Optimization". NASA Glenn Research Center. 2018.

[13] Yoshida, T., "Springback Problems in Forming of High-Strength Steel Sheets and Countermeasures". Nippon Steel Technical Report, 103, pp.390–400. 2013.

[14] Ko, M., and Cora, O., "1 - introduction and state of the art of hydroforming". In Hydroforming for Advanced Manufacturing, M. Ko, ed. Woodhead Publishing, pp. 1 – 29. 2008.

[15] Anggono, A.D., Siswanto, W.A., Omar,B., "Combined Method of Spring-forward and Spring-back for Die Compensation Acceleration". In 4th International Conference on Modeling, Simulation and Applied Optimization. 2018.

[16] Leger, J. Menger Curvature and Rectifiability. *Annals of Mathematics, 149*(3), second series, 831-869. 1999.

[17]Saleh, R., Ali, G. and El-Megharbel, A., "Springback of I-Section Beam after Pure Bending with von Mises Criteria". World Journal of Engineering and Technology, 6, 104-118. 2018.

[18] "C75S, 1.1248, C75 - SPRING STEEL." [Online]. Available:https://virgamet.com/c75s-1-1248-ck75-c75-xc75-xc70-75cr1-aisi-1075-spring-steel.

[19] Sarker, Pratik, "Investigation of the Quenching Characteristics of Steel Components by Static and Dynamic Analyses". *University of New Orleans Theses and Dissertations*. 1942. 2014.

A design

A.1 U-beams

A Finite Element Analysis model was used to determine the parameters of the design as explained in Section 2 of the paper.

The simulation is a simplified model where the result does not depend on the cross sectional shape. Only the stiffness in the z and y directions(figure A.1 as well as the torsional rigidity is used as a parameter. The value of the stiffness can be tweaked to achieve approximately zero-stiffness in rotation. From the stiffnesses in the z and y directions, and the torsional rigidity, the dimensions of the U-section could be determined. The following equations are used to determine the dimensions of the U-section.

The centroid distance y_o can be expressed in the dimensions of the U-section

$$y_o = \frac{1}{A}\left(\frac{(B - 2 \cdot t_f) \cdot t_w^2}{2} + t_f \cdot H^2\right), \tag{A.1}$$

where the area A of the U-section is given in the following equation.

$$A = 2 \cdot H \cdot t_f + (B - 2 \cdot t_f) \cdot t_w \tag{A.2}$$

The moment of inertia of the U-section in the y direction can be written as

$$I_y = \frac{H \cdot B^3}{12} - \frac{(H - t_w) \cdot (B - t_f)^3}{12} \tag{A.3}$$

The moment of inertia of the U-section in the z direction can be written as

$$I_z = \frac{2 \cdot t_f \cdot H^3 + (B - 2 \cdot t_f) \cdot t_w^3}{3} - A \cdot y_o \tag{A.4}$$

The torsional rigidity of the U-section can be written as

$$J = \frac{2 \cdot t_f \cdot H^3 + (B - 2 \cdot t_f) \cdot t_w^3}{3} \tag{A.4}$$
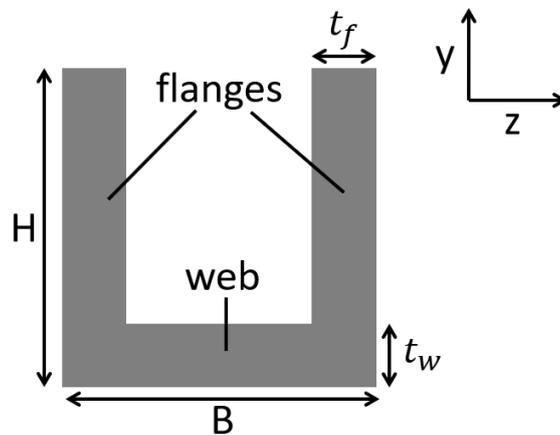
Figure A.1. Design parameters of the U cross-section

A.2 Ansys simulation

An Ansys simulation was performed to analyse the stresses in the U-beams. Figure A.2a shows the beam in prestressed state. Figure A.2b shows a close up of the bottom of the beam where the highest stresses occur.

(a)

(b)
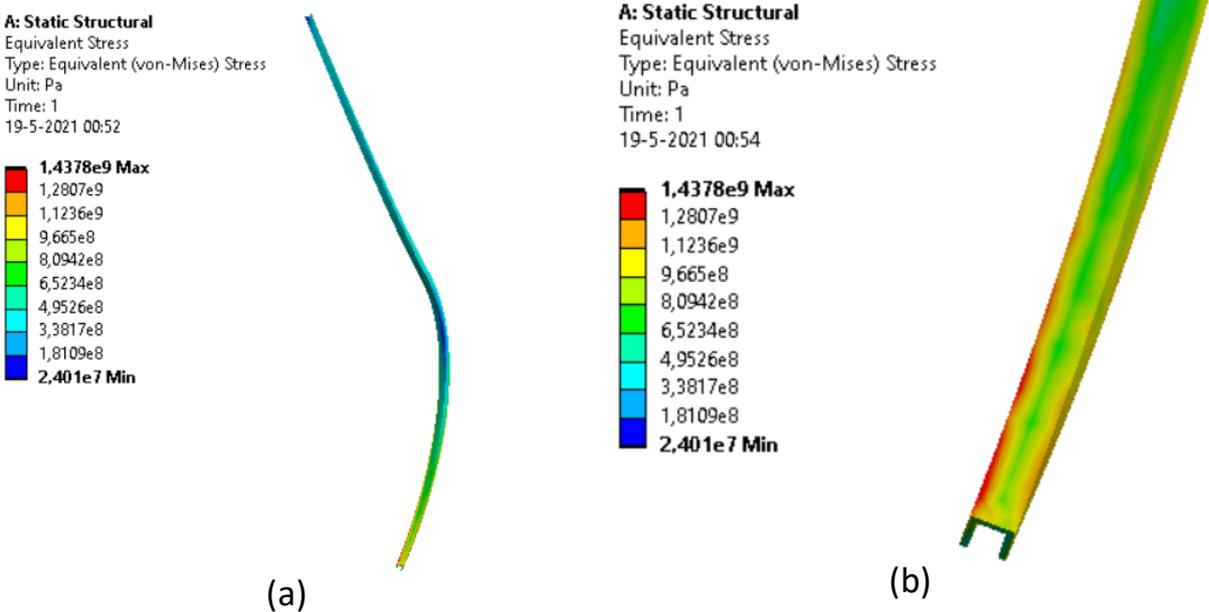
Figure A.2. (a) Ansys simulation of the U-beam in prestressed state. (b) Close up of bottom of the beam

B Manufacturing

B.1 Straight U-beam

Multiple manufacturing techniques have been attempted and analysed which could potentially produce straight thin walled U-beams. By folding a metal sheet twice, a U-profile could be made as illustrated in Figure B.1. This method has been tried with a folding machine and a v-press brake at IMS at the TU delft. The main problem with this method was the lack of precision of the bending line. Also, it is very difficult to bend a sheet with such small dimensions.
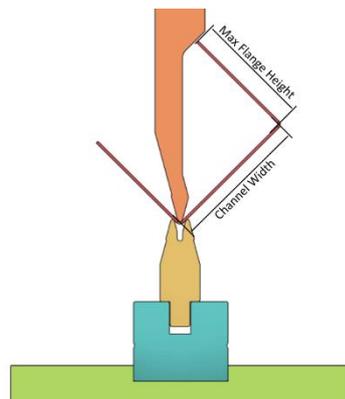
Figure B.1. *Illustration of the production of a U-beam with v-press braking*

Milling with a standard end mill was also tried to produce straight U-beams following the same steps as described in the paper. Milling with an end mill generates a lot of heat, resulting in a lot of thermal deviation of the material as shown in Figure 2. A mill of only 1.5 mm was required to mill the gap of the U-section. A 1.5 mm end mill is very fragile and tends to break very quickly. That is also why it is very time-consuming, because the feed rate and the increments had to be very low to prevent damage to the end mill.

B.2 Heat treatment

The heat treatment of the beam was performed at the Material Science Department at 3Me(TU Delft). Figure B.2a shows the oven that was used. Gloves and a mask were used for safety due to the high temperatures. A large gripper was used to move the beams in and out of the oven, see Figure B.3. Two different heat treatments were performed: quenching and tempering.

Quenching:

First the beam is heated to 840 Celsius. A small hole was drilled at the top of the beam where an iron wire was threaded through. This way, it was possible to grab the beam without damaging when it was 840 Celsius. After heating for about 2 minutes, when the beam had a uniform red colour, the beam is quenched in an oil bath(see Figure B.2b). The beam had to be moved into the oil bed as fast as possible. It has a large influence on the material properties when the beam is at room temperature even for a few seconds after it is heated to 840 degrees. Figure B.4 show this influence where a mistake was made during the quenching process so that the beam was in open air at room temperature for a couple of seconds. A large decrease in strength was observed compared to a beam which is placed in oil as fast as possible (approximately 0.5 seconds).

Tempering:

Tempering was done at 480 Celsius for different tempering times. After the beam was heated, it was placed in a bin filled with sand. This was done to reduce the cooling rate of the beam.

Figure B.5 shows a beam in untreated state, after quenching(hardened) and after tempering.

(a)   (b)
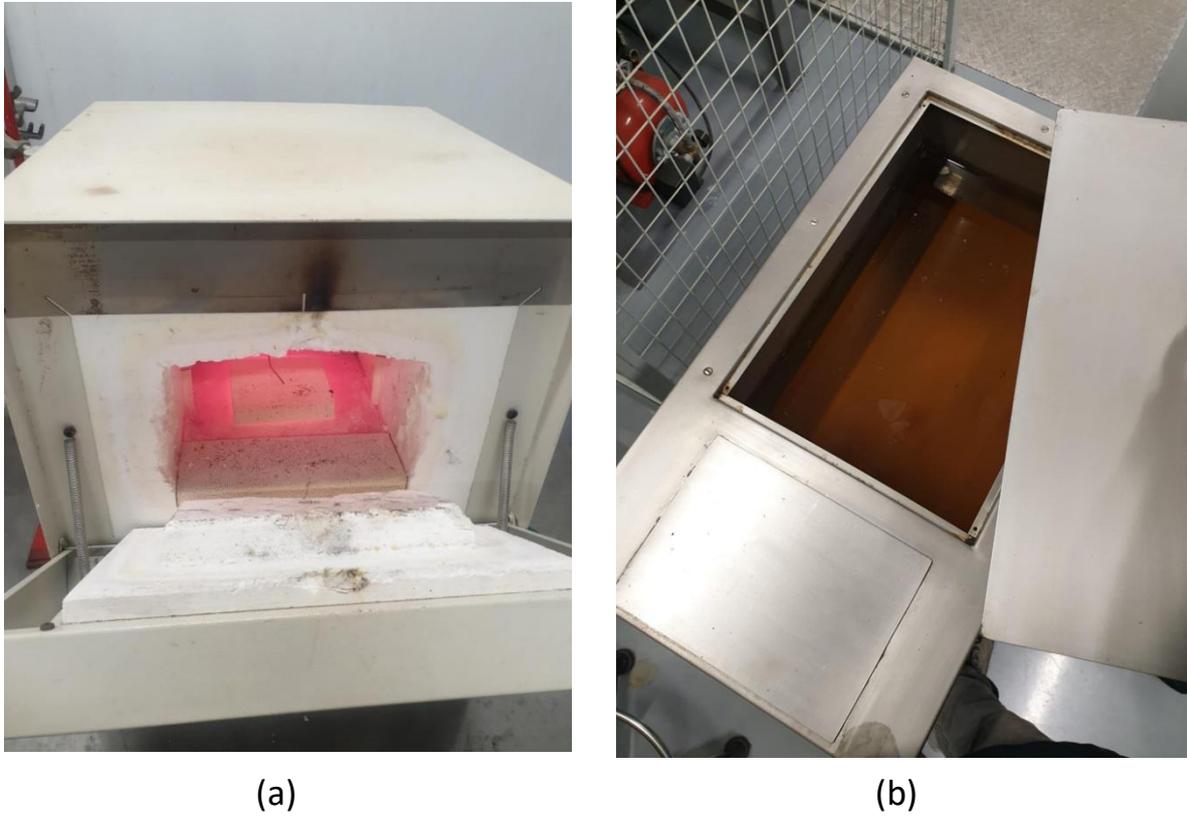
Figure B.2. *(a) Oven used for heating and tempering. (b) Oil bath used for quenching*

Figure B.3. *Safety gear and gripper used to perform the heat treatments*
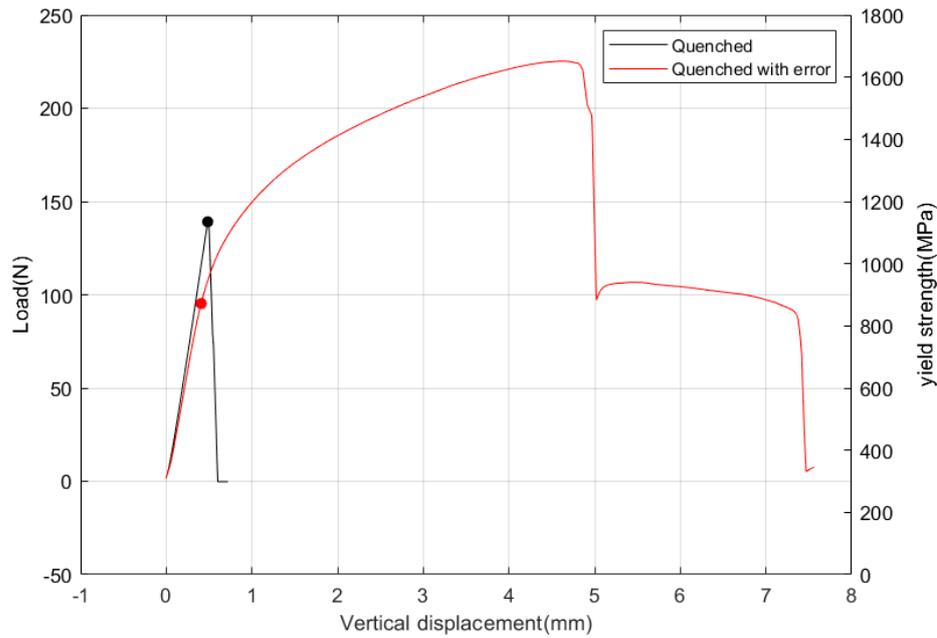
Figure B.4. *Result of three-point bending test for a successfully quenched beam(about 0.5 sec in open air) and a beam which was in open air for a couple of seconds due to an human error.*

Figure B.5. *Result of a untreated, hardened(quenched) and tempered beam.*

B.4 Assembled mechanism

The assembled mechanism consists of an upper connecting body, two lower clamps and two U-beams produced by following the manufacturing method explained, see Figure B.4. The upper connecting body and two lower clamps were 3D printed. The two lower clamps are connected to each other with only one rod. This was done so that the neutral pose of the assembled mechanism could be adjusted. Small manufacturing errors of the beams lead to a distortion in the neutral pose of the mechanism. These errors could be compensated by rotating the clamps independently over the rod which was done with an adjusting screw at one clamp. The rotation applied was very low, but influences the neutral pose significantly.

C implementation die design method

C.1 Extended formulas for springback

This section contains the extended equations of the springback ratio for the three cases explained in section 3.3.3 of the paper.

The springback ratio for case (1), where the yield point h^* is in the upper part of the flange of the U-section between h_2 and h_3 (Figure 9) can be written as

$$
\frac{R_0}{Rf} = \frac{R_0\,(v^2-1)\left(\frac{4\,E\,tf\left(tw-\frac{h^2\,tf+\frac{tw^2\,(b-2\,tf)}{2}}{2\,h\,tf+tw\,(b-2\,tf)}\right)^3}{3\,R_0\,(v^2-1)} - \frac{E\left(tw-\frac{h^2\,tf+\frac{tw^2\,(b-2\,tf)}{2}}{2\,h\,tf+tw\,(b-2\,tf)}\right)^3(b+2\,tf)}{3\,R_0\,(v^2-1)} + \frac{2\,E\,R_0^2\,tf\,(v^2-1)^2}{3\left(\frac{K}{E}\right)^{\frac{3}{n-1}}(v^2-v+1)^{3/2}} - \frac{E\,(b+2\,tf)\left(h^2\,tf+\frac{tw^2\,(b-2\,tf)}{2}\right)^3}{3\,R_0\,(2\,h\,tf+tw\,(b-2\,tf))^3(v^2-1)} - \frac{2\left(\frac{4}{3}\right)^{\frac{n+1}{2}}K\,tf\left(\left(\frac{R_0\,(v^2-1)\left(\frac{E}{K}\right)^{\frac{1}{n-1}}}{\sqrt{v^2-v+1}}\right)^{n+3}-\left(h-\frac{tf\,h^2+\left(\frac{b}{2}-tf\right)tw^2}{2\,h\,tf+tw\,(b-2\,tf)}\right)^{n+3}\right)}{R_0^{\,n}\,(n+3)} + \frac{2\,E\,tf\left(h^2\,tf+\frac{tw^2\,(b-2\,tf)}{2}\right)^3}{3\,R_0\,(2\,h\,tf+tw\,(b-2\,tf))^3(v^2-1)}\right)}{E\left(\frac{2\,h^3\,tf}{3}+\frac{tw^3\,(b-2\,tf)}{3}-\frac{\left(h^2\,tf+\frac{tw^2\,(b-2\,tf)}{2}\right)^2}{2\,h\,tf+tw\,(b-2\,tf)}\right)} + 1
$$

The springback ratio for case (2), where the yield point h^* is in the web of the U-section between h_1 and h_2 can be written as

$$
\frac{R_0}{Rf} = \frac{R_0\,(v^2-1)\left(\frac{4\,E\,tf\left(tw-\frac{h^2\,tf+\frac{tw^2\,(b-2\,tf)}{2}}{2\,h\,tf+tw\,(b-2\,tf)}\right)^3}{3\,R_0\,(v^2-1)} - \frac{E\left(tw-\frac{h^2\,tf+\frac{tw^2\,(b-2\,tf)}{2}}{2\,h\,tf+tw\,(b-2\,tf)}\right)^3(b+2\,tf)}{3\,R_0\,(v^2-1)} + \frac{E\,R_0^2\,(v^2-1)^2\,(b+2\,tf)}{3\left(\frac{K}{E}\right)^{\frac{3}{n-1}}(v^2-v+1)^{3/2}} + \frac{2\frac{1}{\left(\frac{3}{4}\right)^{\frac{n+1}{2}}}K\,tf\left(\left(h-\frac{h^2\,tf+\frac{tw^2\,(b-2\,tf)}{2}}{2\,h\,tf+tw\,(b-2\,tf)}\right)^{n+3}-\left(\frac{h^2\,tf+\frac{tw^2\,(b-2\,tf)}{2}}{2\,h\,tf+tw\,(b-2\,tf)}\right)^{n+3}\right)}{R_0^{\,n}\,(n+3)} + \frac{\left(\frac{4}{3}\right)^{\frac{n+1}{2}}K\left(\left(\frac{tf\,h^2+\left(\frac{b}{2}-tf\right)tw^2}{2\,h\,tf+tw\,(b-2\,tf)}\right)^{n+3}-\left(\frac{R_0\,(v^2-1)\left(\frac{E}{K}\right)^{\frac{1}{n-1}}}{\sqrt{v^2-v+1}}\right)^{n+3}\right)(b+2\,tf)}{R_0^{\,n}\,(n+3)}\right)}{E\left(\frac{2\,h^3\,tf}{3}+\frac{tw^3\,(b-2\,tf)}{3}-\frac{\left(h^2\,tf+\frac{tw^2\,(b-2\,tf)}{2}\right)^2}{2\,h\,tf+tw\,(b-2\,tf)}\right)} + 1
$$

And the springback ratio for case (3), where the yield point h^* is between the neutral axis and the web of the U-section which is between the neutral axis and h_1 can be written as

$$
\frac{R_0}{Rf} = \frac{R_0\,(v^2-1)\left(\frac{4\,E\,R_0^2\,tf\,(v^2-1)^2}{3\left(\frac{K}{E}\right)^{\frac{3}{n-1}}(v^2-v+1)^{3/2}} + \frac{2\frac{1}{\left(\frac{3}{4}\right)^{\frac{n+1}{2}}}K\,tf\left(\left(h-\frac{h^2\,tf+\frac{tw^2\,(b-2\,tf)}{2}}{2\,h\,tf+tw\,(b-2\,tf)}\right)^{n+3}-\left(\frac{h^2\,tf+\frac{tw^2\,(b-2\,tf)}{2}}{2\,h\,tf+tw\,(b-2\,tf)}\right)^{n+3}\right)}{R_0^{\,n}\,(n+3)} + \frac{4\left(\frac{4}{3}\right)^{\frac{n+1}{2}}K\,tf\left(\left(\frac{tf\,h^2+\left(\frac{b}{2}-tf\right)tw^2}{2\,h\,tf+tw\,(b-2\,tf)}-tw\right)^{n+3}-\left(-\frac{R_0\,(v^2-1)\left(\frac{E}{K}\right)^{\frac{1}{n-1}}}{\sqrt{v^2-v+1}}\right)^{n+3}\right)}{R_0^{\,n}\,(n+3)} + \frac{\frac{1}{\left(\frac{3}{4}\right)^{\frac{n+1}{2}}}K\left(\left(\frac{h^2\,tf+\frac{tw^2\,(b-2\,tf)}{2}}{2\,h\,tf+tw\,(b-2\,tf)}\right)^{n+3}-\left(\frac{h^2\,tf+\frac{tw^2\,(b-2\,tf)}{2}}{2\,h\,tf+tw\,(b-2\,tf)}-tw\right)^{n+3}\right)(b+2\,tf)}{R_0^{\,n}\,(n+3)}\right)}{E\left(\frac{2\,h^3\,tf}{3}+\frac{tw^3\,(b-2\,tf)}{3}-\frac{\left(h^2\,tf+\frac{tw^2\,(b-2\,tf)}{2}\right)^2}{2\,h\,tf+tw\,(b-2\,tf)}\right)} + 1
$$

C.2 Implementation

The die design method explained in section 3.3.3 of the paper is implemented in MATLAB. Only case 1 is used in this implementation because the yield point was between the neutral axis and h_1 at all nodes along the curve of the beam. An imaginary node $P(-1)$ was used to determine the curvature at the first node $P(0)$ of the curve, because the two neighbouring nodes are required to determine the radius of curvature. This node was estimated using node $P(0)$ and $P(1)$. This was also done for the last node of the curve.

D experiments

D.1 Curvature measurements

A picture of the curved beams was taken and analysed in MATLAB using the Image processing toolbox and the curvature of the beam could be reproduced by saving roughly 30 mouse click coordinates (x, y). The result of the computed curvature at every node resulted in a lot of noise. This had probably to do with the relatively low quality of the picture. It was hard to click along the curve of the beam due to the low resolution of the picture. This could simply be improved by using a high resolution camera.

D.2 Moment-angle experiment

Figure D.1 shows the resulting moment-angle graph including all the data points of the experiment explained in section 3.5 of the paper. The forces were measured every 50ms and a photo was taken every 400ms. One data point is the determined position of the mechanism using the photo and the mean of 8 force measurements around this point.

The forces when a translation is applied from 0 to 50 mm in the positive y-direction were also measured in another experiment which is not included in the paper. During the translation, the mechanism is kept as straight as possible. Figure D.2 shows the result of this experiment compared with the simulation of the Finite Element Analysis of the model. The curve approximately follows the simulated curve up to a translation of 35mm
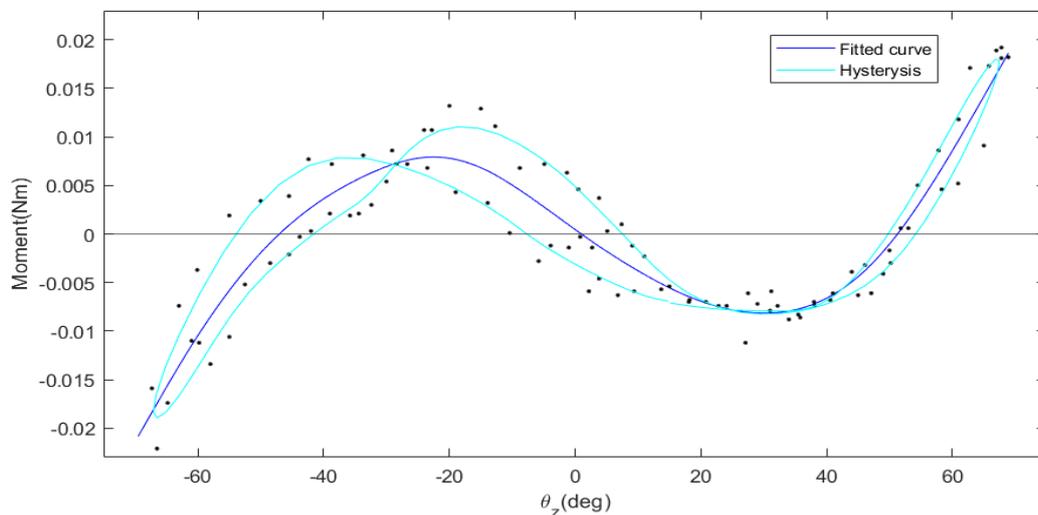
Figure D.1. *The moment-angle curve of the experiment including the hysteresis and the black dotted data points*
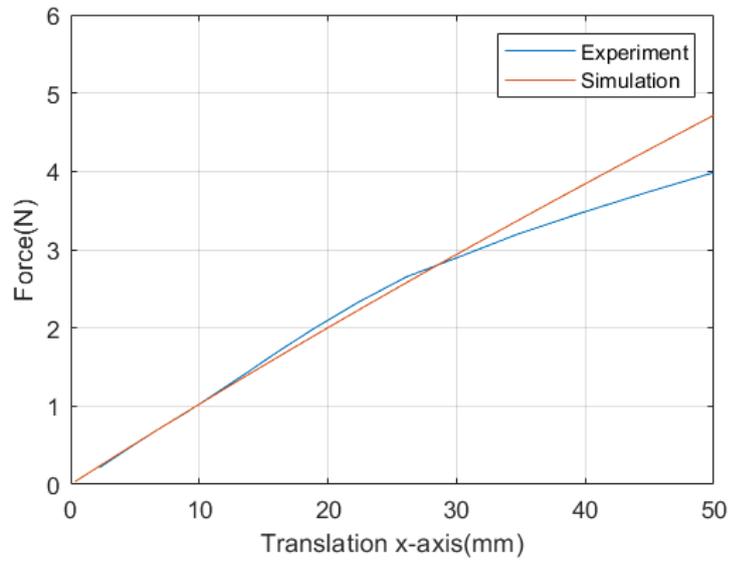
Figure D.1. *The force translation curve of the experiment and the simulation)*

E matlab

E.1 BendingToolshape

```matlab
nodes=500;

%% caculate radius of curvature R from model for every node
R=[];
M=zeros(3,nodes-1);
k=zeros(3,nodes-1);


for i=2:nodes-1

    [R(i),M(1:3,i),k(1:3,i)] =  circumcenter(m_beams.X(i-
1,1:3),m_beams.X(i,1:3),m_beams.X(i+1,1:3));

    if(k(1,i)<0)
        R(i)=-R(i);
     else
        R(i)=R(i);
    end
end
R(1)=R(2);
plot(1./R)


%%

%model data points
x_model=m_beams.X(1:nodes,1);
y_model=m_beams.X(1:nodes,2);
z_model=m_beams.X(1:nodes,3);

%plot original 3d curvature model

plot3(x_model,y_model,z_model)
axis equal

%%
%calculate distance between nodes
distance=[];
for i=1:nodes-1
    distance(i)=sqrt((x_model(i)-x_model(i+1)).^2+(y_model(i)-
y_model(i+1)).^2+(z_model(i)-z_model(i+1)).^2);
end
%%
%Points for model with the overbended curvature
x_bendingModel=[];
y_bendingModel=[];

%start point
x_bendingModel(1)=0;
y_bendingModel(1)=0;
```

```matlab
for i=1:nodes-1
    if(i==1) %first gues point with imiginairy number on the
negative x axis of x_bendingModel, and distance(i-1)=distance.

    beta1=acos((distance(i)/2)/R(i));
    beta2=acos((distance(i)/2)/R(i));

    gamma1=-0.58;
    gamma2=pi-beta1-beta2;
    gamma1_2=gamma1+gamma2;

    x23=distance(i)*cos(gamma1_2);
    y23=distance(i)*sin(gamma1_2);

    x_bendingModel(i+1)=x23;
    y_bendingModel(i+1)=y23;

    elseif(i>1)


    beta1=acos((distance(i-1)/2)/abs(R(i)));
    beta2=acos((distance(i)/2)/abs(R(i)));

    gamma1=atan((y_bendingModel(i)-y_bendingModel(i-
1))/(x_bendingModel(i)-x_bendingModel(i-1)));
    gamma2=pi-beta1-beta2;

    if(R(i)>=0)
    gamma1_2=gamma1+gamma2;
    else
    gamma1_2=gamma1-gamma2;
    end

    x23=distance(i)*cos(gamma1_2);
    y23=distance(i)*sin(gamma1_2);

    x_bendingModel(i+1)=x_bendingModel(i)+x23;
    y_bendingModel(i+1)=y_bendingModel(i)+y23;

    end
end




%% calculate R for compensations springback
R_springback=[];
for i=1:nodes-1
    R_springback(i)=springbackFunction(abs(R(i)));
end

%%
%Points for model with the overbended curvature
x_bendingModel_new=[];
y_bendingModel_new=[];
```

```matlab
%start point
x_bendingModel_new(1)=0;
y_bendingModel_new(1)=0;


for i=1:nodes-1
    if(i==1) %first gues point with imiginairy number on the
negative x axis of x_bendingModel, and distance(i-1)=distance.

    beta1=acos((distance(i)/2)/R_springback(i));
    beta2=acos((distance(i)/2)/R_springback(i));

    gamma1=-0.8;%orientation angle
    gamma2=pi-beta1-beta2;
    gamma1_2=gamma1+gamma2;

    x23=distance(i)*cos(gamma1_2);
    y23=distance(i)*sin(gamma1_2);

    x_bendingModel_new(i+1)=x23;
    y_bendingModel_new(i+1)=y23;

    elseif(i>1)


    beta1=acos((distance(i-1)/2)/abs(R_springback(i)));
    beta2=acos((distance(i)/2)/abs(R_springback(i)));

    gamma1=atan((y_bendingModel_new(i)-y_bendingModel_new(i-
1))/(x_bendingModel_new(i)-x_bendingModel_new(i-1)));
    gamma2=pi-beta1-beta2;

    if(R(i)>=0)
    gamma1_2=gamma1+gamma2;
    else
    gamma1_2=gamma1-gamma2;
    end

    x23=distance(i)*cos(gamma1_2);
    y23=distance(i)*sin(gamma1_2);

    x_bendingModel_new(i+1)=x_bendingModel_new(i)+x23;
    y_bendingModel_new(i+1)=y_bendingModel_new(i)+y23;

    end
end

writematrix([x_bendingModel'.*1000,y_bendingModel'.*1000,zeros(500,1
)],"BendingtoolCoordinatesOriginal.txt","Delimiter","tab");
writematrix([x_bendingModel_new'.*1000,y_bendingModel_new'.*1000,zer
os(500,1)],"BendingtoolCoordinates.txt","Delimiter","tab");

plot(x_bendingModel*1000,-
y_bendingModel*1000,x_bendingModel_new*1000,-
y_bendingModel_new*1000,'r')
legend("Curvature beam","Die shape")
```

```matlab
axis equal
set(gcf,'color','w');
ylim([0 45])
xlabel('Length of beam(mm)')
ylabel('Height of beam(mm)')
```

E.2 Springbackfunction

```matlab
%return radius which compensates the springback for the desired
radius
%Rf=desired radius
%R0=bending radius
Rf=Rf*1000;
syms R0

%geometry
h_u=2.5;
b_u=2.32;
t_u=0.44;
A_u=2*h_u*t_u+(b_u-2*t_u)*t_u;
y_u0=1/A_u*(((b_u-2*t_u)*t_u^2)/2+t_u*h_u^2);
%geometry

%material properties
Ys=423.5e6;%yield strength
E=210e9;%modules of elasticity
K=0; %strength coefficient
n=0.2; %hardening exponent
v=0.29; %poisson ratio


%%

%formula plastic deformation only in flange R0/Rf2
R0_Rf1=1-(1/(1-beta*alpha.^3))*( (3*(1-
v.^2))/(((3/4).^((1+n)/2))*(n+2)) * ((2*R0/H).^(1-n)) * ((Ys/E).^(1-
n)) - (beta * alpha^3)+((2*R0/H).^3) * ((Ys/E).^3) * (((1-
v.^2)^3)/((1+v.^2-v)^(3/2)) - (3*(1-
v.^2).^(n+3))/((3/4).^((1+n)/2)*(n+2)*(1-v+v.^2)^((n+2)/2))));
%formule plastic deformation in flange and web R0/Rf2
%only used this case for the function, R0_Rf1 is only for very
larger radia
R0_Rf2=1-(1/(1-beta*alpha.^3))*( (3*(1-
v.^2))/(((3/4).^((1+n)/2))*(n+2)) * ((2*R0/H).^(1-n)) * ((Ys/E).^(1-
n))*(1-beta*alpha.^(n+2)) +((2*R0/H).^3) * ((Ys/E).^3)*(1-beta) *
(((1-v.^2).^3)/((1+v.^2-v).^(3/2)) - (3*(1-
v.^2).^(n+3))/((3/4).^((1+n)/2)*(n+2)*(1-v+v.^2).^((n+2)/2))));

R2=vpasolve(R0/Rf==R0_Rf2)/1000;
return
```

E.3 GetCoordinates curvature beams

```matlab
I = imread('3C.jpg');
imshow(I);
axis on;
button = 1;

n = 0;
while true
zoom on;
pause() % you can zoom with your mouse and when your image is okay,
you press any key
zoom off;
    [xclick, yclick, button] = ginput(1);
    if isempty(xclick) || button(1) ~= 1; break; end
    n = n+1;
    x(n) = xclick(1); % save all points you continue getting
    y(n) = yclick(1);
    hold on
end

plot(x,y)

angle=atan((y(1)-y(2))/(x(2)-x(1)));
distanceReal=187.3;
distancePoints=sqrt((x(2)-x(1))^2+(y(2)-y(1))^2);
scale=distanceReal/distancePoints;

R = [cos(angle) -sin(angle); sin(angle) cos(angle)];
% Rotate your point(s)

x_trans=x-x(1);
y_trans=y-y(1);

coordinates=[x_trans;y_trans];
coordinates_rotated=R*coordinates;

coordinates_scaled=coordinates_rotated*scale;

x_corrected=coordinates_scaled(1,:);
y_corrected=coordinates_scaled(2,:);


x_final=linspace(x_corrected(1),x_corrected(2),100);
y_final=spline(x_corrected,y_corrected,x_final);
figure(2)
```